JOHN'S NEWFOUNDEAND PANADA

Circulation Patterns

in the

Gulf of St. Lawrence: June 1968 and September 1969

by

F. K. Keyte and R. W. Trites

FISHERIES RESEARCH BOARD OF CANADA

TECHNICAL REPORT NO. 271

1971

FRB

FISHERIES RESEARCH BOARD OF CANADA

Technical Reports

FRB Technical Reports are research documents that are of sufficient importance to be preserved, but which for some reason are not appropriate for primary scientific publication. No restriction is placed on subject matter and the series should reflect the broad research interests of FRB.

These Reports can be cited in publications, but care should be taken to indicate their manuscript status. Some of the material in these Reports will eventually appear in the primary scientific literature.

Inquiries concerning any particular Report should be directed to the issuing FRB establishment which is indicated on the title page.

FISHERIES RESEARCH BOARD OF CANADA TECHNICAL REPORT NO. 271

CIRCULATION PATTERNS IN THE

GULF OF ST. LAWRENCE: JUNE 1968 AND SEPTEMBER 1969

by

F. K. KEYTE1 and R. W. TRITES2

¹Marine Sciences Branch Department of the Environment Atlantic Oceanographic Laboratory Bedford Institute, Dartmouth, N.S.

²Fisheries Research Board of Canada Department of the Environment Marine Ecology Laboratory Bedford Institute, Dartmouth, N.S.

TABLE OF CONTENTS

	Page
ABSTRACT	1
INTRODUCTION	1
BACKGROUND	2
METHOD OF OBSERVATIONS	2
RESULTS	
I. Cruise 3368 (a) Phase 1	3
(b) Phase 2	5
Thermograph Record	6
Current Meter Records	7
Temporal variation of temperature and salinity at a point	7
II. Cruise 69-051	7
Temporal variation of temperature and salinity at a point	10
Current Meter Record	10
CONCLUSIONS	11
ACKNOWLEDGEMENTS	11
REFERENCES	12
LIST OF FIGURES	15
LIST OF TABLES	20

CIRCULATION PATTERNS IN THE

GULF OF ST. LAWRENCE: JUNE 1968 AND SEPTEMBER 1969

ABSTRACT

Data from two cruises undertaken to investigate circulation patterns in the Gulf of St. Lawrence south of Anticosti Island, indicate good correlation between the drift of subsurface parachute drogues and the surface geopotential anomalies, within a time span of 2-3 days.

INTRODUCTION

Two cruises spaced 15 months apart were recently undertaken by the Bedford Institute to look at circulation patterns in the Gulf of St. Lawrence. The areas were chosen to overlap and extend the 1964 and 1965 surveys by Blackford (1965a, 1967), in the area between Cape Breton Island, Prince Edward Island and Anticosti Island. Figure 1 shows the boundaries of the two earlier surveys and the two described here.

Data gathered in physical oceanographic investigations in the Gulf area have considerable interest for biologists. Part of the field of inquiry investigated by all four cruises to a greater or lesser extent was to relate, if possible, circulation patterns and plankton distributions. Do clockwise gyres (closed contours in the mass field flow pattern) enclose or retain the plankton populations? If so, it may in turn be that some fish populations would congregate in the gyres to feed. Alternately, counterclockwise gyres may result in nutrient-rich deeper water being brought into the euphotic zone. In June 1968 two ships, the Canadian Scientific Ship DAWSON on cruise number 3368, and the Motor Vessel BRANDAL on cruise number 3668 sampled a rectangular grid of stations in the

Magdalen Shallows area; DAWSON was concerned primarily with gathering temperature and salinity data, while the BRANDAL concentrated on taking vertical and horizontal plankton tows. In September 1969 the DAWSON made a rectangular grid survey in the Gaspé Passage area (cruise number 69-051). Only the physical oceanographic results of the two DAWSON cruises are reported here.*

BACKGROUND

Circulation studies in the Gulf of St. Lawrence have been reported by Blackford (1965a, 1965b, 1967), Bumpus and Lauzier (1965), Farquharson (1962, 1963, 1966), Forrester (1967), Lauzier (1965, 1967), Lawrence (1968), MacGregor (1956), Murty (1968), Trites and Ewing (1963), and Trites (1963). The general features that emerge are that fresher water outflows along the Gaspe coast and through the Cape Breton side of Cabot Strait, while saltier water inflows on the Anticosti side of the Gaspe Passage and on the Newfoundland side of Cabot Strait. There appears to be no large net flow through the Strait of Belle Isle. A map of the overall geopotential anomalies reveals a gyre south of Anticosti Island (El Sabh et al, 1969). A brief summary of the physical oceanographic features has been given by Trites (1970).

METHOD OF OBSERVATIONS

Cruises 3368 and 69-051 occupied oceanographic stations with an STD (salinity-temperature-"depth", actually pressure) sensor and measuring system designed by the National Research Council and built by

* Some results of the biological study have been reported in "Zooplankton, Summary Report No. 10, Canadian Oceanographic Identification Centre, National Museum of Natural Sciences, Ottawa". Guildline Instruments, Ontario. The sea unit which weighs about 20 kg in air, measures the three variables as d-c voltages to a shipboard analog graphical output and digital tape recorder. Temperatures and salinities at desired pressures were read off the graphs manually. On cruise 69-051 the use of a Hewlett-Packard 9100A calculator allowed the geopotential anomaly to be obtained shortly after each station, whereas geopotential anomalies were not available for cruise 3368 till some weeks after its completion. We estimate the accuracy of pressure to be about ± 0.1 dbar, temperature $\pm 0.03^{\circ}$ C, and salinity ± 0.03 .

A Lagrangian view of the currents at 10 metres below the surface and at 40 metres was obtained using parachute drogues, 7.3 metres in diameter, set at these levels, and supported by floats. A floating radio beacon tied to the float, together with a flashing light and radar reflector on the float itself, helped the ship to locate the drogues at intervals during the criss-crossing of the grids.

RESULTS

I. Cruise 3368 (a) Phase 1

The layout of the grid of stations set out for the cruise is shown in Figure 2. For convenience the rows of the grid are labelled with numerals, the columns with letters. The latitudes of the rows and longitudes of the columns are given in Table 1. Altogether there were 172 stations occupied, some grid points being sampled once, others twice and a few three times. Table 2 shows the correspondence between station numbers and grid points, along with GMT times when the station was taken. Figure 3 illustrates the sequence of the first 67 stations (which are referred to as Phase 1 of this cruise) from Station 1 at grid point 9G to 67 at 1A; four extra stations were generated because of a detour from 9E to 7E to moor two current meters and two thermographs.

After station 5 at 7E we proceeded to station 6 at 7D, 7 at 8D, 8 at 9D, and then resumed Row 9 (Fig. 3).

The elapsed time between Station 1 and Station 67 was about 3½ days, which means that the contours and isopleths drawn for this phase of the cruise (See Figs. 4-7, 9-12) are synoptic only within this time scale. Of course, this problem of the synoptic value of patterns drawn on an oceanographic grid has been the source of much discussion in the literature, and a few comments on this point are made at the end of this report.

Surface isotherms and isohalines of Cruise 3368, Phase 1, are drawn in Figs. 4 and 5. Warmer, fresher water lies in the western part of the grid, with colder, saltier water to the **no**rtheast. The gradients of the isopleths on the surface are weak if compared with the gradients at 20 dbar (Figs. 6 and 7). The warm fresh water is still seen at 20 dbar in the western edge of the grid, but elsewhere the pattern is complex. Some of the reason for this is undoubtedly that the thermocline was normally very sharp (several degrees/dbar) and was usually centered at about 20 m depth.

We made the assumption that the 20 dbar temperature plot would, in the absence of a computational facility to obtain geopotential anomalies, provide a sensitive indicator of gyres. It was assumed that flow would be along the isotherms, with warm water to the right, hence from Fig. 6 we concluded at the time that there was a dominant flow from northeast to south-southeast, a smaller area where water was moving to the northeast and a zone between these two flows where the motion was feeble and very weak gyres were present.

Subsurface drogues were laid at grid points, 3D, 4F, 5B, 5D, 5F, 7D, 7E and midway between 7E and 7F. The tracks of these droques are shown in Fig. 8, with six-digit (day-hour-minutes) GMT times of release and sightings plotted, as well as calculated average speeds between sightings. In Fig. 9, the droque tracks are shown superimposed on the outline of the 20 dbar isotherm pattern of Fig. 6. The drogues moved with some relation to the southerly flow, but elsewhere there is little correspondence with the northeast flow depicted by the isotherms. Thus it was interesting to compute and plot the geostrophic current pattern (some weeks after the cruise) using surface geopotential anomalies relative to an assumed level of no motion at 40 dbars (Fig. 10). These contours were replotted over the subsurface droque tracks (Fig. 11) with remarkably good results for the flow direction. The average drogue speeds from Fig. 8 may be compared with the geostrophic speeds obtained by using the inset nomogram in Fig. 10. Comparison of the two speeds suffers from the lack of frequent sightings of the drogues; nevertheless, there appears to be relatively good agreement. In order to validate the choice of 40 dbar as the reference level of no motion, several drogues were set at this level, with results shown in Fig. 12. While motions are much less than at the surface, currents still appear to be somewhat higher than desirable at the reference level.

Vertical cross-sections of temperature and salinity for Rows 1-9 of this Phase are shown in Figs. 13-22.

(b) Phase 2

With the completion of Station 67 at 1A the DAWSON steamed through the grid taking several stations on the way back to grid point 96.

Station 76 was taken at 9G at 1925Z on 25/6/68, after which the grid was retraversed as far as Row 3. In the meantime, drogue motions had been largely to the south, so reoccupation of Rows 2 and 1 was abandoned. Instead, the ship proceeded directly south from 3A (Station 124) to 7A (Station 125), thence on a crenelated route to 12K (Station 172). The grid for Phase 2 is shown in Fig. 23.

For comparison with Figs. 4-7, we show surface isotherms and isohalines (Figs. 24, 25) and 20 dbar isotherms and isohalines (Figs. 26,27) of Phase 2. Some smoothing of the data has been done for the second and third occupations of grid points along Row 9. We also show the subsurface drogue tracks superimposed on the Phase 2 20 dbar isotherm pattern (Fig. 28) and note the poor correlation. On the other hand the geopotential anomalies of Phase 2 (Fig. 29) fit the drogue track pattern well (Fig. 30).

Vertical cross-sections of temperature and salinity for Rows 3-12 of Phase 2 are drawn in Figs. 31-43.

Thermograph Record

The two thermographs moored at Station 5 i.e. at grid point
7E on the Bradelle Bank, took readings every 20 minutes beginning at
2140 GMT on 18/6/68. The shallow instrument was at 12 m, the deep one
at 45 m. Readings ceased at approximately 1740 GMT on 27/6/68, giving
a record of nearly nine days. Tables 3 and 4 list the 20-minute
readings at 12 m and 45 m, while Fig. 44 shows 4-hour, 12-hour and 24-hour
averages of the readings. The shallower traces show some fluctuation,
but the deeper trace has amplitudes of only about 0.5°C.

Current Meter Records

Two current meters, at 13 m and 44 m were laid at grid point 7E (Station 5) at 2140 GMT on June 18th, and recovered at 1330 GMT June 28th. The two films were read and processed, first into current speed, or rate (cm/sec) and true direction (Fig. 45), then into resolved N-S, E-W components (Fig. 46). The major and minor components are quite similar, and seem in reasonable agreement with the current speeds at the surface and at 40 m as measured by the parachute drogues (Figs. 8, 12). Unfortunately the immersion time of only 9½ days does not permit one to accurately remove the tidal constituents.

Temporal variation of temperature and salinity at a point

During the evening of June 25th, 1968, while at grid position 12E (Station 148), the STD was lowered nine times in succession in order to record the vertical variations in temperature and salinity over a short period of time. The first STD drop was at 260235 GMT; the last at 260235 GMT. The records of the first, third, fifth, seventh, and ninth traces are illustrated in Fig. 48. Fluctuations are rather heavily influenced by the thermo/halocline, but even so one sees fluctuations in the top ten metres amounting to about 0.2°C magnitude. Some of the fluctuations in the depth of the thermocline were periodic in character and were the result of internal waves. Their amplitude however was usually not more than 2-3 metres.

II. Cruise 69-051

The area chosen for this cruise is shown in Figure 49. A rectangular grid was set up, with latitudes of the rows, and longitudes of the columns, listed in Table 5. Seventy-three stations comprised the grid. The correspondence between grid position and station number

is listed in Table 6. A second run over the grid could not be completed, and yielded only three more stations: 88 at 3A, 89 at 3B, and 90 at 3C.

The reference level for geopotential anomalies was chosen to be 200 dbar, with the view to providing a better approximation to a level of no motion. The geopotential anomalies of the surface relative to 200 dbar are drawn in Figure 50, and the tracks of the two subsurface (10 m depth) drogues released, one at 4B (Station 24) and the other at 5D (Between Stations 87 and 88) are superimposed on the contours in Figure 51. The track of the only deeper drogue released (40 m at 4B) is also shown in this figure. It was recovered over a week after release, with its antenna broken. The NNW-moving drogue was not recovered; the time shown (302200) was when the DAWSON hove to about \(^12\) mile from the shore of Anticosti Island in the first of two recovery attempts. Clearly, the drogue could have grounded earlier than this, but the average speed of 0.4 knots is based on 302200 as the "recovery" time.

The correspondence between directional drift and average speed of the subsurface drogues and the current speed and direction deduced from the contours is good. One notes that the time scale of this grid is in the order of 2-3 days. On the other hand, the geopotential anomalies available from the beginning of the second traverse of the grid show a major shift in the pattern of contours around 3A - 3C. The time period between the two occupations of 3A was 4 days, which suggests that the "synopticity" of Figure 50 was less than this. Contours of geopotential anomalies drawn up for grids with time scales longer than 4 days (e.g. Trites, 1963) probably smooth out many of the fluctuations in the shape of gyres or smaller eddies.

It is probably worth noting that if the reference level for this cruise had been chosen as 40 dbar, the geopotential anomaly contours would have shown features similar to the 200 dbar level, but would not have proved so accurate a predictor of drogue motion (See Fig. 52).

Surface isotherms (Fig. 53) and isohalines (Fig. 54), 20 dbar isotherms (Fig. 55) and isohalines (Fig. 56) and 40 dbar isotherms (Fig. 57) and isohalines (Fig. 58) reflect, to some extent, the features seen in the geopotential anomaly topography. One notes the cooler saltier tongue of water lying NNW-SSE from the western end of Anticosti, paralleling the geopotential anomaly trough in that location, and also the warmer fresher pool in the southern part of the grid, paralleling the geopotential anomaly ridge there.

We have also examined the pattern of isohalines on specific potential density surfaces (Carr, 1937). Figure 59 shows the salinity distribution and pressure field of the σ_{\odot} = 25.5 surface, chosen because it is under the thermocline and hence removed from the effects of the upper mixed layer. Figures 60 and 61 are salinity and pressure distributions on the σ_{\odot} = 26.0 and σ_{\odot} = 27.0 surfaces respectively. Areas of closed isohalines on isopycnal surfaces, or more generally areas where isohalines run up or down pressure gradients, may indicate vertical motion (Carr, op. oit). Such motion may then be occurring at 4C, 9C and 10B in Figure 32, and 5E in Figure 61, for example. Also, comparison between Figures 60 and 61 shows the greater activity on the deeper surface. Isohaline gradients, and differences between maximum and minimum closed isohalines, are very much weaker on σ_{\odot} = 26.0 and on σ_{\odot} = 27.0. The maximum salinity difference on

the former surface is 0.07% (9K to 9C-9D); on the latter surface it is 0.18% (6F to 7K).

From Figure 61 there are indications of currents carrying saltier water northwestward along the Anticosti coast; and parallel but some miles farther south, currents carrying fresher water southeastward.

Vertical cross-sections of temperature and salinity are illustrated for Rows 2-10 (Figs. 62-76), and for the diagonal line 10B-5G (Figs. 77, 78).

Temporal variation of temperature and salinity at a point

At four stations along the grid there were multiple STD drops to examine temporal temperature fluctuations at a particular point. For example, Station 39 (grid position 6F) was occupied at 240937, 240954, 241015 and 241030 GMT. The four temperature and salinity traces are reproduced in Figure 79. Below the thermocline, the amplitude of the temperature oscillations is seen to reach about 0.9C at 192 dbar; in the thermocline the excursion is large (perhaps up to several degrees) at any particular pressure because of the very steep temperature gradient there. The amplitude of the salinity oscillations reaches about 0.5% at 205 dbar.

Current Meter Record

Although not formally planned to be part of the circulation study, one current meter was moored off English Point, Gaspé Peninsular, on 19/9/69, at a depth of 15 m. Results are shown in Fig. 80. Peak current speeds were about 130 cm/sec (2.5 kt), average speed was about 60 cm/sec (1.2 kt). There is a curious fluctuation in direction for the

first 12 days of the record; then (except for a fluctuation on day 17) the direction settles down to a fairly steady 130° .

CONCLUSIONS

During two cruises in the Gulf of St. Lawrence in the area south of Anticosti Island, surface currents seemed to correspond to currents indirectly calculated by the geostrophic method, even though the time period covered by the indirect method was 2-3 days. When longer periods were examined, the synoptic assumption seemed to become untenable.

The question remains of the dominant period of temperature and salinity oscillations at any one point within the Gulf area, with respect to the one-hour time span between grid stations. The evidence suggests that short-period oscillations at a point are not significant in the scale size of the grid, particularly since the surface currents are themselves the result of motions averaged over periods of many hours.

ACKNOWLEDGEMENTS

We wish to acknowledge the assistance of John Lord, Peter Coady, George Taylor and Roger Belanger for the illustrations (Figs. 1-80), and to the scientific staff, officers and crew of the two DAWSON cruises 3368 and 69-051. We also thank colleagues at Bedford Institute for valuable discussions.

REFERENCES

Blackford, B. L. 1965 a. A simple two-dimensional electrical analog model for wind-driven circulation in the Gulf of St. Lawrence.

Fish. Res. Bd. Canada. Unpubl. MS Report (Ocean and Limn.)

Series No. 185, 48 pp.

1965 b. Some oceanographic observations in the southeastern Gulf of St. Lawrence - summer 1964. Ibid., No. 190, 22 pp.

1967. Some oceanographic observations in the southern Gulf of St. Lawrence - summer 1965. Fish. Res. Bd. Canada, Unpubl. Tech. Report Series No. 26, 34 pp.

- Bumpus, D. F. and L. M. Lauzier 1965. Surface circulation on the

 Continental Shelf off Eastern North America between Newfoundland
 and Florida. Serial Atlas of the Marine Environment Folio 7,
 American Geogr. Soc., N. Y.
- Carr, A. E. 1937. Isopycnic analysis of current flow by means of identifying properties. J. Mar. Res., 1, 133-154.
- E1-Sabh, M. I., W. D. Forrester and O. M. Johannessen 1969.

 Bibliography and some aspects of physical oceanography in the
 Gulf of St. Lawrence. McGill University, Marine Sciences

 Centre Manuscript Report No. 14.
- Farquharson, W. I. 1962. Tides, tidal streams and currents in the

 Gulf of St. Lawrence. Canada Dept. Mines and Technical Surveys,

 Marine Sciences Branch, 76 pp.

1963. Gaspe Passage current and oceanographic survey, 1962. Bed. Inst. Oceanogr., Dartmouth, N. S., Canada. Unpubl. MS for internal circulation No. 63-9.

1966. St. Lawrence Estuary current surveys. Bed.
Inst. Oceanogr., Dartmouth, N. S., Canada. Unpubl. MS Report
66-6, 84 pp.

- Forrester, W. D. 1967. Currents and geostrophic currents in the St. Lawrence Estuary. Bed. Inst. Oceanogr. Dartmouth, N.S. Canada. Unpubl. MS Report 67-5, 175 pp.
- Lauzier, L. M. 1965. Drift bottle observations in Northumberland
 Strait, Gulf of St. Lawrence. J. Fish. Res. Bd. Canada, 22 (2):
 353-368.
 - 1967. Bottom residual drift on the Continental Shelf area of the Canadian Atlantic coast. J. Fish. Res. Bd. Canada 24 (9): 1845-1859.
- Lawrence, D. J. 1968. Current meter data from Cabot Strait, 1966.

 Atlantic Oceanogr., Lab., Bed. Inst., Dartmouth, N. S.

 Canada BI Data Series 68-10-D.
- MacGregor, D. G. 1956. Currents and transport in Cabot Strait. J. Fish. Res. Bd. Canada, 13 (3): 435-448.
- Murty, T. S. 1968. Wind-induced circulation and flow pattern models.
 In Gulf of St. Lawrence Workshop, Bed. Inst., Dartmouth, N. S.
 Canada, pp. 28-32.

Trites, R. W. 1963. Geostrophic flow in the Gulf of St. Lawrence.

Fish Res. Bd. Canada, Atlantic Oceanogr. Group, Bed. Inst.

Oceanogr., Dartmouth, N. S. Annual Report and Investigators
summaries, 1962-63, pp. 34-35.

1970. The Gulf of St. Lawrence from a pollution viewpoint. FAO Technical Conference on marine pollution and its effects on living resources and fishing. Rome, December 1970, Doc. FIR:MP/70/R-18 (23 pp.).

Trites, R. W. and G. N. Ewing 1963. Variation in temperature and salinity structure in Gaspe Passage. Fish. Res. Bd. Canada, Atlantic Oceanogr. Group, Bed. Inst. Oceanogr., Dartmouth, N.S. Annual Report and Investigators summaries, 1962-63, pp. 38-39.

LIST OF FIGURES

- Fig. 1. Surveys of 1964, 1965, 1968 and 1969.
- Fig. 2. Location of grid points for Cruise 3368, June 1968; Phase 1 18th-22nd,
 Phase 2 22nd-27th.
- Fig. 3. Phase 1 of Cruise 3368. Station 1 was at 9G, Station 67 at 1A.

 See Table 2.
- Fig. 4. Surface temperatures, Cruise 3368, Phase 1.
- Fig. 5. Surface salinities, Cruise 3368, Phase 1.
- Fig. 6. 20 dbar temperatures, Cruise 3368, Phase 1.
- Fig. 7. 20 dbar salinities, Cruise 3368, Phase 1.
- Fig. 8. Tracks of subsurface (10 m) parachute drogues, and calculated average speeds between sightings, Cruise 3368.
- Fig. 9. Tracks of subsurface drogues superimposed on 20 dbar Phase 1 isotherms: Cruise 3368.
- Fig. 10. Geopotential anomalies, dynamic centimetres relative to 40 dbar,
 Cruise 3368, Phase 1.
- Fig. 11. Tracks of subsurface buoys superimposed on Phase 1 geopotential anomalies, Cruise 3368.
- Fig. 12. Tracks of 40-metre parachute drogues, and calculated average speeds between sightings, Cruise 3368.
- Fig. 13. Temperature (top) and salinities (bottom) cross-section, Row 9,
 Cruise 3368, Phase 1.
- Fig. 14. Temperature (top) and salinity (bottom) cross-section, Row 8,
 Cruise 3368. Phase 1.
- Fig. 15. Temperature (top) and salinity (bottom) cross-section, Row 7,

 Cruise 3368, Phase 1.

- Fig. 16. Temperature (top) and salinity (bottom) cross-section, Row 6, Cruise 3368, Phase 1.
- Fig. 17. Temperature (top) and salinity (bottom) cross-section, Row 5, Cruise 3368, Phase 1.
- Fig. 18. Temperature (top) and salinity (bottom) cross-section, Row 4, Cruise 3368, Phase 1.
- Fig. 19. Temperature (top) and salinity (bottom) cross-section, Row 3, Cruise 3368, Phase 1.
- Fig. 20. Temperature (top) and salinity (bottom) cross-section, Row 2, Cruise 3368, Phase 1.
- Fig. 21. Temperature cross-section, Row 1, Cruise 3368, Phase 1.
- Fig. 22. Salinity cross-section, Row 1, Cruise 3368, Phase 1.
- Fig. 23. Phase 2 of Cruise 3368. See Table 2, Stations 76-172.
- Fig. 24. Surface temperatures, Cruise 3368, Phase 2.
- Fig. 25. Surface salinities, Cruise 3368, Phase 2.
- Fig. 26. 20 dbar temperatures, Cruise 3368, Phase 2.
- Fig. 27. 20 dbar salinities, Cruise 3368, Phase 2.
- Fig. 28. Tracks of subsurface drogues superimposed on Phase 2 20-dbar isotherms Cruise 3368.
- Fig. 29. Geopotential anomalies, dynamic centimetres relative to 40 dbar Cruise 3368, Phase 2.
- Fig. 30. Tracks of subsurface buoys superimposed on geopotential anomalies Cruise 3368, Phase 2.
- Fig. 31. Temperature (top) and salinity (bottom) cross-section, Row 3, Cruise 3368, Phase 2.

- Fig. 32. Temperature (top) and salinity (bottom) cross-section, Row 4, Cruise 3368, Phase 2.
- Fig. 33. Temperature (top) and salinity (bottom) cross-section, Row 5, Cruise 3368, Phase 2.
- Fig. 34. Temperature (top) and salinity (bottom) cross-section, Row 6, Cruise 3368. Phase 2.
- Fig. 35. Temperature (top) and salinity (bottom) cross-section, Row 7, Cruise 3368, Phase 2.
- Fig. 36. Temperature (top) and salinity (bottom) cross-section, Row 8, Cruise 3368, Phase 2.
- Fig. 37. Temperature (top) and salinity (bottom) cross-section, Row 9, Cruise 3368, Phase 2.
- Fig. 38. Temperature cross-section, Row 10, Cruise 3368, Phase 2.
- Fig. 39. Salinity cross-section, Row 10, Cruise 3368, Phase 2.
- Fig. 40. Temperature cross-section, Row 11, Cruise 3368, Phase 2.
- Fig. 41. Salinity cross-section, Row 11, Cruise 3368, Phase 2.
- Fig. 42. Temperature cross-section, Row 12, Cruise 3368, Phase 2.
- Fig. 43. Salinity cross-section, Row 12, Cruise 3368, Phase 2.
- Fig. 44. Readings from thermographs submerged at (a) 12m and (b) 45m, at grid position 7E, Bradelle Bank, Cruise 3368. Twenty minute readings have been here averaged over 4-hour, 12-hour and 24-hour periods.

 Starting date 18/6/68. See Tables 3 and 4.
- Fig. 45. Currents (rate and true direction) at 13m(top) and 44m (bottom)

 Cruise 3368. Mooring lay was completed at 2140Z on 18/6/68;

 mooring recovery was completed at 1330Z on 28/6/68. See text.

- Fig. 46. Currents at station 5, resolved into plus major component North, minus major component South, Cruise 3368.
- Fig. 47. Currents at station 5, resolved into plus minor component East, minus minor component West, Cruise 3368.
- Fig. 48. Temporal variation in vertical temperature (top) and salinity (bottom) readings, Station 148 grid position 12E, Cruise 3368, Phase 2.
- Fig. 49. Location of grid points for Cruise 69-051, June 23-27, 1969.
- Fig. 50. Geopotential anomalies, dynamic centimetres, relative to 200 dbar, Cruise 69-051.
- Fig. 51. Movement of two subsurface (10m) drogues and one 40m drogue (recovered, antenna broken) superimposed on geopotential anomalies relative to 200 dbar. (For explanation of numbers, see Fig. 8).

 DAWSON reached south coast of Anticosti Island at 2200 GMT on Sept. 30 but beached drogue could not be recovered.
- Fig. 52. Geopotential anomalies, dynamic centimetres, relative to 40 dbar, Cruise 69-051.
- Fig. 53. Surface temperatures, Cruise 69-051.
- Fig. 54. Surface salinities, Cruise 69-051.
- Fig. 55. 20 dbar temperatures, Cruise 69-051.
- Fig. 56. 20 dbar salinities, Cruise 69-051.
- Fig. 57. 40 dbar temperatures, Cruise 69-051.
- Fig. 58. 40 dbar salinities, Cruise 69-051.
- Fig. 59. Isohalines % (solid lines, 4 digits) and pressure field, dbar (dashed lines, italic digits) on σ_{Θ} = 25.5 surface, Cruise 69-051.
- Fig. 60. Isohalines% (solid lines, 4 digits) and pressure field dbar (dashed lines, italic digits), on σ_{α} = 26.0 surface, Cruise 69-051.
- Fig. 61. Isohalines%(solid lines, 4 digits) and pressure field, dbar (dashed lines, italic digits) on σ_{Θ} = 27.0 surface, Cruise 69-051.

- Fig. 62. Temperature (left) and salinity (right) cross-section of Row 2, Cruise 69-051.
- Fig. 63. Temperature (left) and salinity (right) cross-section of Row 3, Cruise 69-051.
- Fig. 64. Temperature (left) and salinity (right) cross-section of Row 4, Cruise 69-051.
- Fig. 65. Temperature cross-section, Row 5, Cruise 69-051.
- Fig. 66. Salinity cross-section, Row 5, Cruise 69-051.
- Fig. 67. Temperature cross-section, Row 6, Cruise 69-051.
- Fig. 68. Salinity cross-section, Row 6, Cruise 69-051.
- Fig. 69. Temperature cross-section, Row 7, Cruise 69-051.
- Fig. 70. Salinity cross-section, Row 7, Cruise 69-051.
- Fig. 71. Temperature cross-section, Row 8, Cruise 69-051.
- rig. 71. Temperature cross-section, Now o, cruise 09-051.
- Fig. 72. Salinity cross-section, Row 8, Cruise 69-051.
- Fig. 73. Temperature cross-section, Row 9, Cruise 69-051.
- Fig. 74. Salinity cross-section, Row 9, Cruise 69-051.
- Fig. 75. Temperature cross-section, Row 10, Cruise 69-051.
- Fig. 76. Salinity cross-section, Row 10, Cruise 69-051.
- Fig. 77. Temperature cross-section, Diagonal 10B-9C-8D-7E-6F-5G, Cruise 69-051.
- Fig. 78. Salinity cross-section, Diagonal 10B-9C-8D-7E-6F-5G, Cruise 69-051.
- Fig. 79. Temporal variations in vertical temperature (top) and salinity (bottom) traces, Station 39, grid position 6F, Cruise 69-051.
- Fig. 80. Current meter record for English Point September 1969. The Station number (52) does not relate to the station numbers of the grid (Fig. 49).

LIST OF TABLES

- Table 1. Grid positions, Cruise 3368.
- Table 2. Station numbers, grid positions and times GMT (day, hour, minutes): Cruise 3368, 18/6/68 - 27/6/68.
- Table 3. Thermograph readings, 12m, grid position 7E. Readings run from left to right, top to bottom, and occur every 20 minutes. Start time 2140 GMT 18/6/68 (reading of 14.5°C). See Figure 44.
- Table 4. Thermograph readings, 45m, grid position 7E. Start time as in Table 3. See Figure 44.
- Table 5. Grid positions, Cruise 69-051.
- Table 6. Station numbers, grid positions and times GMT (day, hour, minutes): Cruise 69-051, 23/9/69 - 27/9/69.

TABLE 1
Grid positions, Cruise 3368

Row	Latitude	Column	Longitude
1	48°25.8'N	A	63°53.5'W
2	48°15.8'N	В	63°38.5'W
3	48°05.8'N	C	63°23.5'W
4	47°55.8'N	D	63°08.5'W
5	47°45.8'N	E	62°53.5'W
6	47°35.8'N	F	62°38.5'W
7	47°25,8'N	G	62°23.5'W
8	47°15.8'N	Н	62°08.5'W
9	47°05.8'N	I	61°53.5'W
10	46°55.8'N	J	61°38.5'W
11	46°45.8'N	K	61°23.5'W
12	46°35.8'N		

Table 2

Station numbers, grid positions and times GMT (day, hour, minutes):

Cruise 3368, 18/6/68 - 27/6/68

S = Station number, G = Grid point, T = Time

S	G	T	S	G	Т	S	G	Т	c	G	Т	
-	-	_			-	- 1	<u>u</u>	-	<u>S</u>	<u>u</u>	-	
1	9G	181600	44	4E	210005	87	8E	230550	130	11B	250820	
2	9F	181800	45	4G	210112	88	8F	230647	131	10B	250925	
3	9E	181905	46	3G	210210	89	8G	230745	132	9B	251018	
4	8E	182030	47	3F	210305	90	7G	230845	133	90	251110	
5	7E	182210	48	3F	210435	91	7F	230942	134	100	251202	
6 7	7D	182345	49	3E	210535	92	7E	231110	135	110	251315	
8	8D 9D	190040 190130	50 51	3D 3C	210730	93	7D	231155	136	120	251405	
9	90	190130	52	3B	210825 210950	94	70	231245	137	12D	251500	
10	9E	190235	53	3B	211045	95 96	7B 7A	231355	138	110	251550	
11	9A	190405	54	2A	211300	96	6A	231600 231805	139	10D 9D	251645 251745	
12	8A	190700	55	2B	211400	98	6B	231904	140	8D	251745	
13	8B	190810	56	20	211500	99	60	232027	142	7D	252020	
14	80	190910	57	2D	211605	100	6D	232135	143	7E	252110	
15	8D	191015	58	2E	211735	101	6E	232230	144	8E	252245	
16	8E	191110	59	2F	211830	102	6F	232340	145	9E	252350	
17	8F	191205	60	2G	211948	103	6G	240033	146	10E	260040	
18	8G	191330	61	1G	212050	104	5G	240125	147	11E	260135	
19	7G	191425	62	1F	212330	105	5F	240258	148	12E	260235	
20	7F	191557	63	1E	220120	106	5E	240410	149	12F	260530	
21	7E	191800	64	10	220245	107	5D	240505	150	11F	260630	
22	7D	191945	65	10	220424	108	5C	240615	151	10F	260725	
23	7C	192143	66	18	220522	109	5B	240720	152	9F	260820	
24	7B	192242	67	1A	220628	110	5A	241005	153	9G	260913	
25	7A	192334	68	3E	221135	111	4A	241110	154	10G	261004	
26	6A	200056	69	*	221215	112	4B	241205	155	11G	261055	
27	6B	200200	70	5F **	221324	113	4C	241335	156	12G	261315	
28	6C 6D	200305 200405	71 72	5F	221409	114	4D	241455	157	12H	261404	
30	6E	200405	73	6F	221508	115	4E 4F	241555	158	11H	261510	
31	6F	200615	74	7F	221715	117	4F 4G	241653 241745	159 160	10H 9H	261610 261725	
32	6G	200715	75	8F	221812	118	3G	241745	161	91	261815	
33	5G	200900	76	9G	221925	119	3F	241940	162	101	261918	
34	5F	201140	77	9F	222015	120	3E	242033	163	111	262017	
35	5E	201235	78	9E	222110	121	3D	242130	164	121	262111	
36	5D	201410	79	9D	222210	122	30	242220	165	12J	262203	
37	5C	201513	80	90	222330	123	3B	242310	166	111	262300	
38	5B	201650	81	9B	230020	124	3A	250005	167	103	262345	
39	5A	201815	82	9A	230115	125	7A	250330	168	91	270100	
40	4A	202010	83	8A	230205	126	8A	250425	169	9K	270155	
41	4B	202113	84	8B	230305	127	9A	250527	170	10K	270245	
42	4C	202205	85	80	230355	128	10A	250625	171	11K	270340	
43	4D	202305	86	8D	230450	129	11A	250720	172	12K	270435	

14.5	14.0	13.0	44 7						2 2		
7.9		12.0	11.7	10.0	9.3	9.1	8.9	8.9	8.0	8.0	8.0
	7.8	7.7	7.6	7.5	7.5	7.6	7.8	8.0	8.0	8.1	8.5
9.0	9.1	9.3	9.5	9.5	9.3	9.4	9.6	9.9	9.8	9.3	9.1
9.1	9.5	9.8	9.7	9.5	9.0	9.0	8.9	8.4	8.0	7.7	7.7
7.8	8.0	8.1	8.2	8.9	9.0	9.7	9.9	9.9	9.9	9.8	9.2
9.0	9.0	9.0	9.0	8.9	8.4	8.3	8.8	9.1	9.0	9.0	9.0
9.0	8.1	8.4	8.8	8.9	9.0	9.3	9.7	9.9	9.9	9.9	9.8
9.6	9.7	9.9	9.9	9.9	9.8	9.1	8.7	8.6	8.7	9.0	9.0
8.5	8.0	8.0	7.9	7.9	7.9	8.0	8.0	8.1	8.2	8.2	8.5
9.1	9.0	8.5	8.1	8.1	8.0	8.0	8.0	8.0	8.0	8.1	8.8
9.0	9.1	9.1	9.1	9.1	9.0	8.9	9.2	9.5	9.6	9.5	9.5
9.4	9.3	9.2	9.1	9.2	9.1	9.0	9.0	9.0	9.1	9.0	8.9
8.0	8.0	7.9	7.9	8.2	8.5	9.0	8.8	8.9	9.0	9.1	9.2
8.0	7.8	7.6	7.6	7.8	7.9	8.1	9.0	9.0	9.0	9.0	9.0
9.0	9.0	9.0	8.5	7.8	7.2	7.0	7.1	7.5	7.9	7.9	7.8
8.0	8.1	8.4	8.7	8.9	9.1	9.0	8.9	8.7	8.5	8.2	8.1
8.1	8.1	8.1	8.0	8.0	8.0	8.0	8.0	8.0	8.0	8.0	8.0
8.0	8.6	8.5	8.5	8.6	8.7	8.8	8.7	8.4	8.3	8.2	8.1
7.9	7.9	7.8	7.8	7.6	7.4	7.2	7.0	7.0	7.1	7.5	7.9
8.1	8.6	8.9	8.7	8.9	8.9	8.7	8.7	8.9	9.0	9.1	9.2
8.9	8.5	8.3	8.7	8.9	8.6	8.4	8.3	8.2	8.1	8.0	8.0
8.0	8.0	8.0	8.1	8.5	8.6	8.5	8.0	8.0	8.0	8.0	8.1
8.2	8.4	8.7	8.9	9.0	9.1	9.4	9.0	8.7	8.6	8.5	8.5
8.5	8.5	8.4	8.2	8.1	8.1	8.1	8.1	9.0	9.5		10.0
10.0	9.8	9.8	10.0	10.1	10.0	9.1	8.9	8.8	8.7	8.6	8.9
9.0	9.0	8.8	8.4	8.2	8.1	8.1	8.0	8.5	9.0	9.2	9.5
9.9	10.0	10.0	10.0	9.9	9.5	8.9	8.9	8.9	8.9	9.0	9.0
9.0	9.0	9.0	9.0	8.9	8.8	9.0	9.8	9.9	9.0	8.9	8.8
8.5	8.2	8.1	8.0	8.0	8.0	8.0	8.0	8.0	8.0	8.0	8.0
8.1	8.1	8.2	8.5	8.8	8.9	9.0	9.3	9.5	9.6	9.7	9.8

Thermograph readings, 12 m, grid position 7E. Readings run from left to right, top to bottom, and occur every 20 minutes. Start time 2140 GMT $\,$ 18/6/68 (reading of 14.5°C). See Figure 44.

9.8	9.4	9.2	9.1	9.0	8.9	8.9	9.0	9.1	9.2	9.7	9.7
9.7	9.7	9.8	9.9	9.9	9.9	9.8	9.5	9.1	8.9	8.5	8.5
8.9	9.0	9.1	8.5	8.4	8.3	.8.2	8.1	8.0	8.0	7.8	7.1
7.0	7.8	7.7	7.1	7.6	8.0	9.0	9.6	9.8	9.8	9.8	9.8
9.7	9.8	9.8	9.8	9.9	10.0	10.0	10.0	10.0	10.0	10.0	10.0
10.0	10.0	10.0	9.9	9.9	9.9	10.0	10.0	10.0	9.9	9.8	9.5
9.4	9.3	9.1	9.0	9.0	9.0	8.5	9.1	9.5	9.8	10.0	10.0
10.0	10.0	10.0	10.0	10.0	9.9	9.8	9.6	9.3	9.1	8.5	8.2
8.2	9.0	9.5	10.0	10.0	10.0	10.1	10.2	10.3	10.2	10.1	9.8
9.0	8.8	8.6	8.9	9.6	9.9	9.9	10.0	10.1	10.4	10.9	10.8
10.0	8.1	7.9	7.7	7.4	7.1	7.0	6.9	6.9	6.8	6.7	6.7
6.7	6.8	6.9	7.0	7.0	7.1	7.5	7.8	8.0	8.5	9.1	9.5
9.6	9.8	9.9	9.7	9.5	9.4	9.2	9.5	9.6	9.1	9.0	9.0
9.0	9.0	9.0	8.0	7.0	7.0	7.8	7.9	8.0	8.1	8.1	8.0
8.0	7.9	7.5	7.5	7.9	8.0	7.5	7.0	7.0	6.9	6.8	6.5
6.7	7.0	7.3	7.7	7.9	8.0	8.0	8.0	8.1	8.2	8.1	8.2
8.3	8.3	8.3	8.2	8.1	8.0	7.9	7.7	7.6	7.6	7.7	7.9
7.9	8.0	8.1	8.1	8.0	7.9	7.9	8.1	8.7	8.9	8.9	8.8
8.5	8.3	8.3	8.1	7.9	7.1	7.0	7.0	7.3	7.6	7.6	7.7
7.8	7.8	7.8	7.8	7.8	7.8	7.5	7.2	7.0	7.0	7.0	7.0
7.0	7.1	7.2	7.3	7.7	7.7	7.6	7.6	7.7	7.7	7.8	7.7
7.0	6.9	6.6	6.6	6.8	7.0	7.2	7.9	7.9	7.9	7.9	7.5
7.3	7.9	8.3	8.5	8.5	8.2	8.0	8.0	8.0	8.0		

Thermograph readings 12 m, grid position 7E. End time 1740 GMT 27/6/68 approx.

0.6	0.2	0.2	0.2	0.2	0.2	0.2	0.2	0.2	0.3	0.2	0.3
0.2	0.2	0.2	0.2	0.2	0.2	0.2	0.2	0.1	0.1	0.1	0.1
0.0	0.0	0.0	0.0	0.0	0.0	0.0	0.0	0.0	0.0	0.0	0.0
0.0	0.0	0.0	0.0	0.0	0.0	0.0	0.0	0.0	0.0	0.0	0.0
0.0	0.0	0.0	0.0	0.0	0.0	0.0	0.0	0.0	0.0	0.0	0.0
0.1	0.1	0.0	0.0	0.0	0.0	0.0	0.0	0.0	0.0	0.0	0.0
0.1	0.1	0.1	0.1	0.1	0.1	0.1	0.1	0.1	0.0	0.0	0.0
0.1	0.2	0.2	0.2	0.1	0.0	0.0	0.0	0.0	0.0	0.0	0.0
0.1	0.1	0.1	0.1	0.1	0.1	0.2	0.2	0.2	0.2	0.2	0.2
0.1	0.1	0.1	0.1	0.2	0.1	0.1	0.1	0.1	0.1	0.1	0.1
0.2	0.1	0.1	0.1	0.2	0.1	0.1	0.1	0.1	0.1	0.1	0.1
0.0	0.0	0.0	0.0	0.0	0.0	0.0	0.0	0.0	0.0	0.0	0.0
0.0	0.0	0.0	0.1	0.1	0.1	0.2	0.2	0.2	0.2	0.2	0.2
0.2	0.3	0.3	0.3	0.3	0.3	0.3	0.3	0.2	0.2	0.2	0.2
0.2	0.3	0.3	0.3	0.3	0.3	0.3	0.3	0.2	0.2	0.2	0.1
0.1	0.0	0.0	0.0	0.0	0.0	0.0	0.0	0.0	0.0	0.0	0.0
0.0	0.0	0.0	0.0	0.0	0.0	0.0	0.0	0.0	0.0	0.0	0.0
0.0	0.0	0.0	0.0	0.0	0.1	0.1	0.0	0.0	0.0	0.0	0.0
0.0	0.0	0.0	0.0	0.0	0.0	0.0	0.1	0.0	0.0	0.0	0.0
0.0	0.0	0.0	0.0	0.0	0.0	-0.1	-0.1	-0.1	-0.1	-0.1	-0.1
-0.2	-0.3	-0.2	-0.2	-0.2	-0.2	-0.3	-0.3	-0.2	-0.2	-0.2	-0.3
-0.3	-0.3	-0.2	-0.2	-0.2	-0.2	-0.2	-0.2	-0.3	-0.3	-0.3	-0.3
-0.4	-0.4	-0.3	-0.3	-0.3	-0.3	-0.2	-0.2	-0.1	-0.2	-0.2	-0.2
-0.1	-0.1	0.0	0.0	0.0	0.0	0.0	0.0	0.0	0.0	-0.1	-0.1
-0.2	-0.2	-0.2	-0.2	-0.2	-0.1	-0.1	-0.1	-0.1	-0.2	-0.2	-0.1
-0.1	-0.1	-0.1	-0.1	-0.1	-0.1	-0.1	-0.1	0.0	0.0	0.0	0.0
0.0	0.0	0.0	0.0	0.0	0.0	0.0	0.0	0.0	0.0	0.0	0.0
0.0	0.0	0.0	0.0	0.0	0.0	0.0	0.0	0.0	0.0	-0.1	-0.1
-0.1	-0.2	-0.2	-0.2	-0.2	-0.1	-0.1	-0.2	-0.2	-0.2	-0.1	-0.1
-0.2	-0.2	-0.2	-0.2	-0.2	-0.2	-0.2	-0.1	0.0	0.0	0.0	0.0

Thermograph readings, 45 m, grid position 7E. Start time as in TABLE 3. See Figure 44.

TABLE 4 (CONTINUED)

0.0	0.0	0.0	-0.1	-0.1	0.0	0.0	0.0	0.0	0.0	0.0	0.0
0.0	0.0	0.0	0.0	0.0	0.0	0.0	0.0	0.0	0.0	0.0	0.0
0.0	0.0	0.0	0.0	0.0	0.0	0.0	0.0	0.0	0.0	0.0	0.0
0.0	0.0	0.0	0.0	0.0	-0.1	-0.1	-0.1	-0.1	-0.1	-0.1	-0.1
-0.1	-0.1	-0.1	-0.1	-0.2	-0.2	-0.2	-0.3	-0.4	-0.4	-0.4	-0.2
-0.2	-0.2	-0.2	-0.2	-0.2	-0.4	-0.3	-0.3	-0.3	-0.4	-0.4	-0.4
-0.4	-0.4	-0.4	-0.4	-0.3	-0.3	-0.3	-0.2	-0.2	-0.1	-0.1	-0.1
0.0	0.0	0.0	0.0	0.0	0.0	0.0	0.0	0.0	0.0	0.0	0.0
0.0	0.0	0.0	0.0	0.0	0.0	0.0	0.0	0.0	0.0	0.0	0.0
0.0	0.0	0.0	0.0	0.0	0.0	-0.1	-0.1	-0.1	-0.1	-0.1	-0.1
-0.1	-0.1	-0.1	0.0	0.0	0.0	0.0	0.0	0.0	0.0	0.0	0.0
0.0	-0.1	-0.1	0.0	0.0	0.0	0.0	0.0	0.0	0.0	0.0	0.0
0.0	0.0	-0.1	-0.1	-0.1	-0.1	-0.1	-0.2	-0.2	-0.2	-0.1	-0.1
-0.1	-0.1	-0.1	-0.1	-0.1	0.0	0.0	0.0	0.0	0.0	0.0	0.0
0.0	0.0	0.0	-0.1	-0.1	-0.1	-0.1	-0.1	-0.1	-0.1	-0.1	-0.2
-0.3	-0.3	-0.3	-0.3	-0.3	-0.3	-0.4	-0.4	-0.4	-0.4	-0.4	-0.4
-0.3	-0.4	-0.4	-0.4	-0.4	-0.4	-0.4	-0.4	-0.4	-0.4	-0.4	-0.4
-0.4	-0.5	-0.5	-0.5	-0.5	-0.5	-0.5	-0.5	-0.5	-0.5	-0.5	-0.5
-0.5	-0.5	-0.5	-0.5	-0.5	-0.5	-0.5	-0.5	-0.5	-0.5	-0.5	-0.5
-0.5	-0.5	-0.5	-0.5	-0.5	-0.5	-0.5	-0.5	-0.6	-0.6	-0.6	-0.2
-0.6	-0.6	-0.6	-0.6	-0.6	-0.6	-0.6	-0.6	-0.6	-0.6	-0.5	-0.5
-0.5	-0.5	-0.5	-0.5	-0.5	-0.6	-0.6	-0.6	-0.6	-0.6	-0.6	-0.6
-0.6	-0.6	-0.6	-0.6	-0.6	-0.5	-0.3	-0.3	-0.3	-0.3	-0.3	-0.3
-0.3	-0.3	-0.3	-0.3	-0.3	-0.3	-0.3	-0.3	-0.3	-0.3	-0.4	-0.5
-0.6	-0.5	-0.4	-0.4	-0.4	-0.5	-0.5	-0.5	-0.5	-0.5	-0.5	-0.3
-0.1	0.0	0.0	0.0	0.0	0.1	0.1	0.1	0.1	0.1	0.1	0.0
-0.1	-0.1	-0.2	-0.3	-0.3	-0.2	-0.2	-0.2	-0.1	-0.1	-0.1	-0.1
-0.1	-0.2	-0.2	-0.2	-0.3	-0.3	-0.3	-0.3	-0.2	-0.1	-0.1	

Thermograph readings, 45 m, grid position 7E. End time as in TABLE 3.

- 26

TABLE 5
Grid positions, Cruise 69-051

Row	Latitude	Column	Longitude
1	49°50' N	A	64°30' W
2	49°40' N	В	64°15' W
3	49°30' N	C	64°00' W
4	49°20' N	D	63°45' W
5	49°10' N	E	63°30' W
6	49°00' N	F	63°15' W
7	48°50' N	G	63°00' W
8	48°40' N	Н	62°45' W
9	48°30' N	I	62°30' W
10	48°20' N	J	62°15' W
	The last of the last of the	K	62°00' W
		L	61°45' W

TABLE 6

Station numbers, grid positions and times GMT (day, hour, minutes): Cruise 69-051, 23/9/69 - 27/9/69

S = Station number, G = Grid point, T = Time

c	c	+	c		-			
<u>s</u>	<u>G</u>	Ī	<u>s</u>	G	Ī	<u>s</u>	G	Ī
15*	1A	230720	40	6G	241118	65	8L	260650
16	2A	230807	41	6H	241300	66	9L	260800
17	2B	230902	42	61	241448	67	9K	260905
18	20	230950	43	6J	241546	68	9J	261007
19	3D	231100	44	6K	241638	69	91	261108
20	30	231148	45	6L	241730	70	9Н	261211
21	3B	231244	46	7L	241882	71	9G	261310
22	3A	231357	47	7K	241843	72	9F	261408
23	4A	231459	48	7J	242040	73	9E	261500
24	4B	231600	49	71	242148	74	9D	261557
25	4C	231727	50	7H	242242	75	90	261648
26	4D	231820	51	7G	242239	76	10A	261942
27	4E	231911	52	7F	250042	77	10B	262039
28	5G	232051	53	7E	250133	78	100	262134
29	5F	232141	54	7 D	250228	79	100	262226
30	5E	232318	55	70	250330	80	10E	262324
31	5D	240013	56	80	252002	81	10F	270032
32	5C	240108	57	8D	252056	82	10G	270145
33	5B	240326	58	8E	252150	83	10H	270258
34	5A	240425	59	8F	252246	84	101	270410
35	6B	240542	60	8G	252348	85	10J	270524
36	6C	240634	61	8H	260109	86	10K	270645
37	6D	240730	62	81	260230	87	10L	270805
38	6E	240840	63	8J	260403	88	ЗА	271948
39	6F	240937	64	8K	260533	89	3B	272121
						90	30	272244

^{*} Stations 1-14 were occupied in an earlier, separate phase of this cruise.

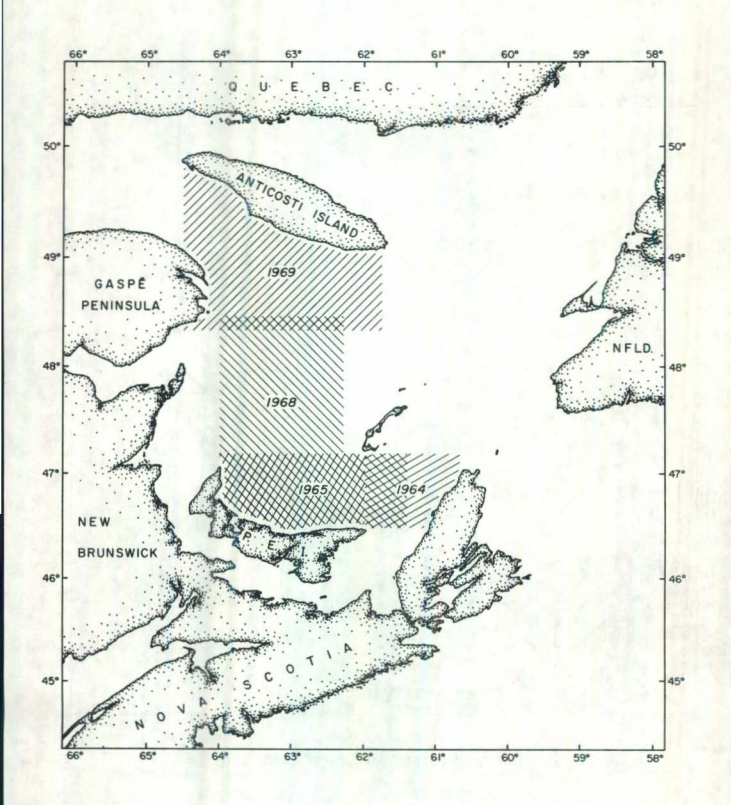
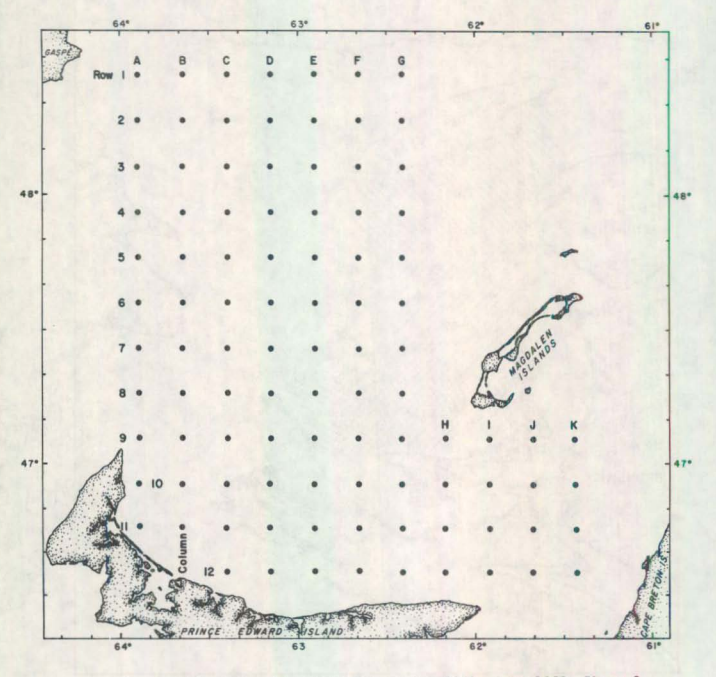


Fig. 1. Surveys of 1964, 1965, 1968 and 1969



g. 2. Location of grid points for cruise 3368, June 1968; Phase 1 18th-22nd, Phase 2 22nd-27th.

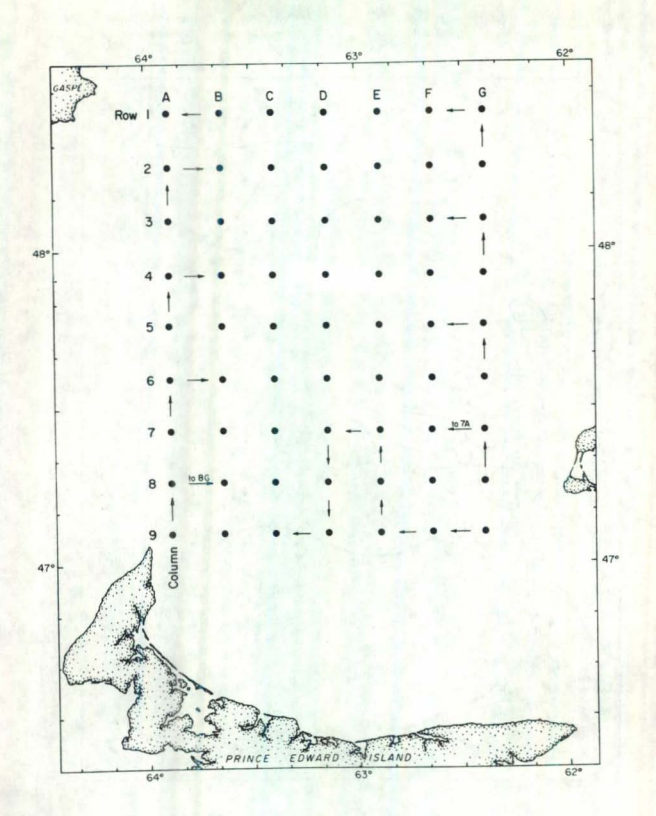


Fig. 3. Phase 1 of Cruise 3368. Station 1 was at 9G, Station 67 at 1A. See Table 2.

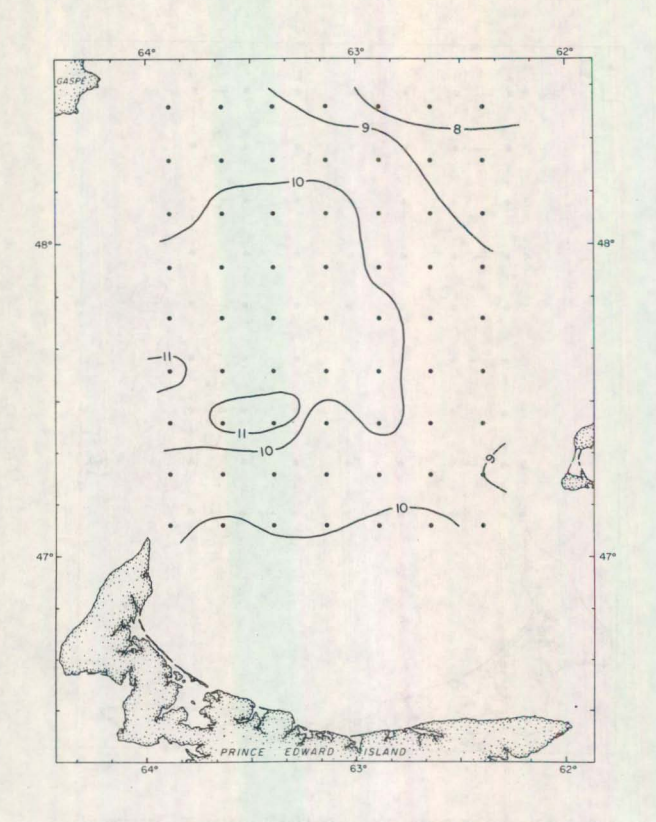


Fig. 4. Surface temperatures, Cruise 3368, Phase 1

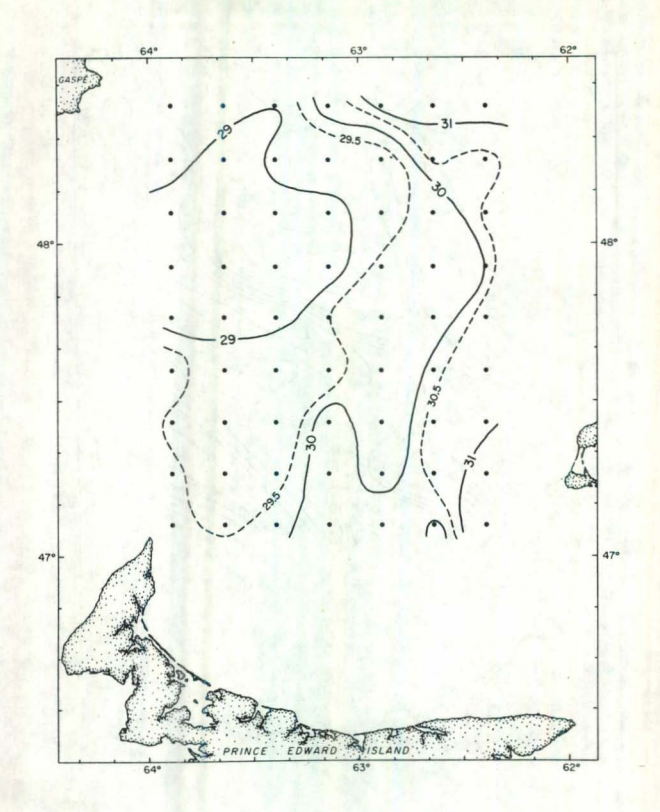


Fig. 5. Surface salinities, Cruise 3368, Phase 1.

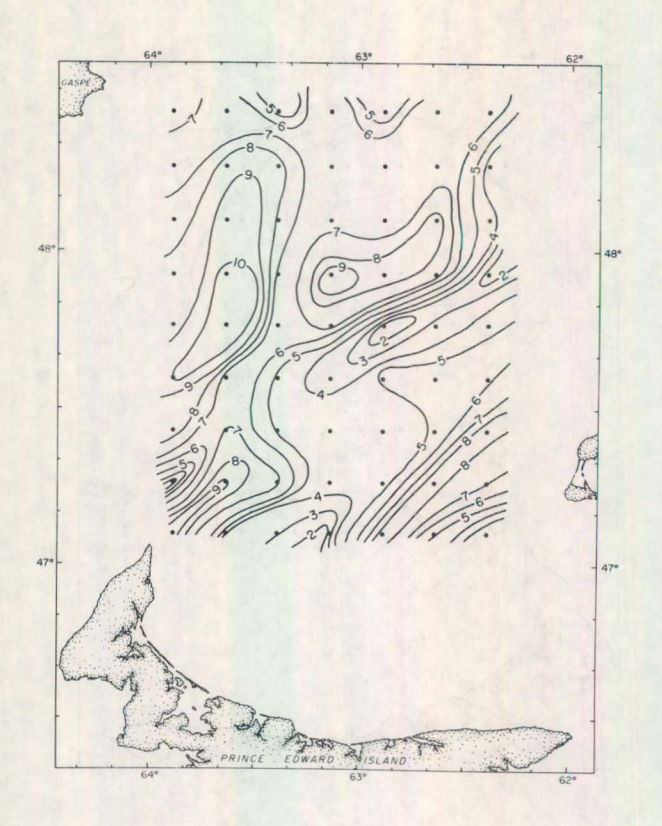


Fig. 6. 20 dbar temperatures, Cruise 3368, Phase 1

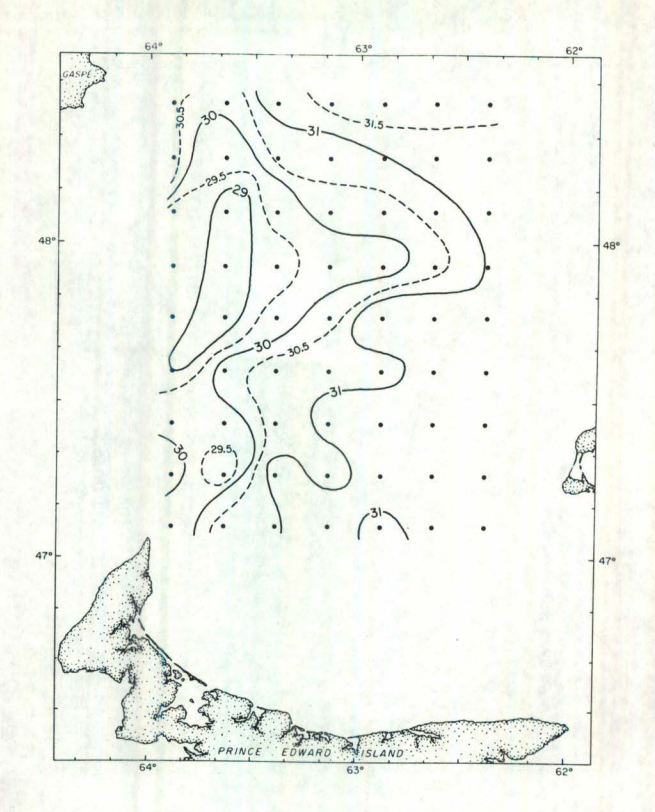


Fig. 7. 20 dbar salinities, Cruise 3368, Phase 1

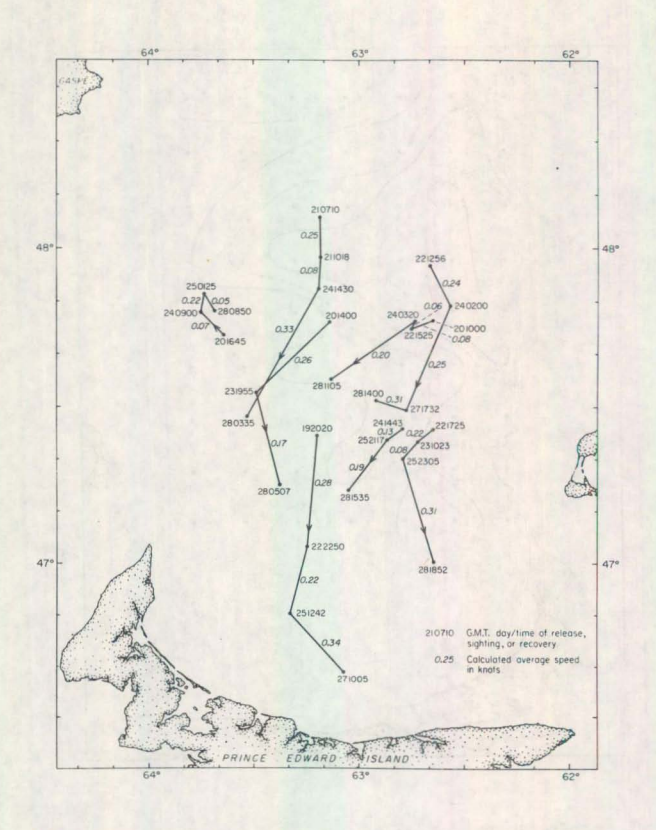


Fig. 8. Tracks of subsurface (10 m) parachute drogues, and calculated average speeds between sightings, Cruise 3368.

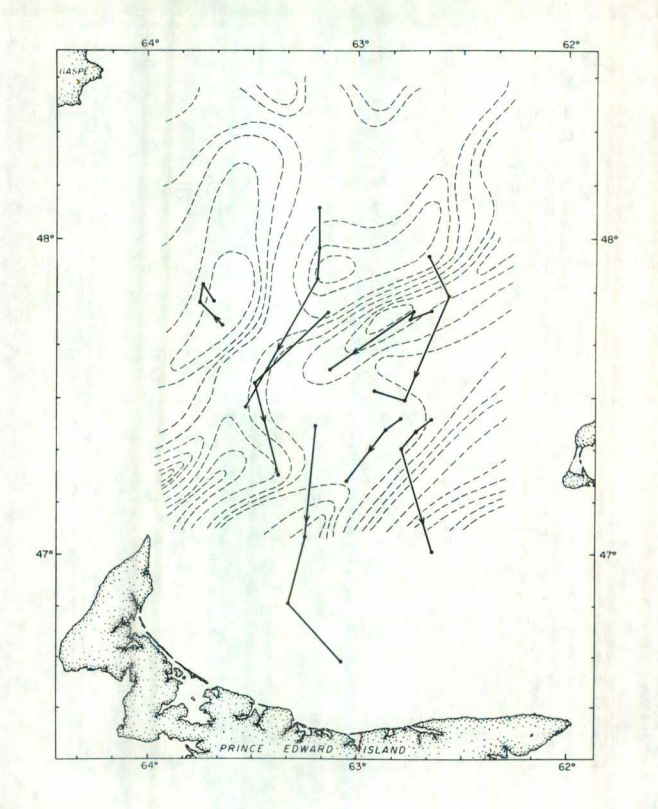


Fig. 9. Tracks of subsurface drogues superimposed on 20 dbar
Phase 1 isotherms; Cruise 3368.

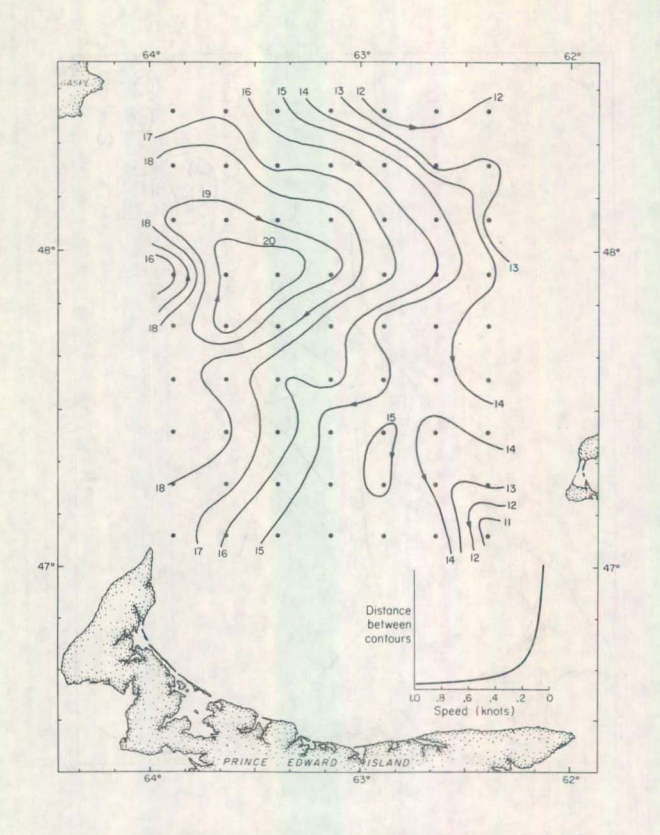


Fig. 10. Geopotential anomalies, dynamic centimetres relative to 40 dbar, Cruise 3368, Phase 1

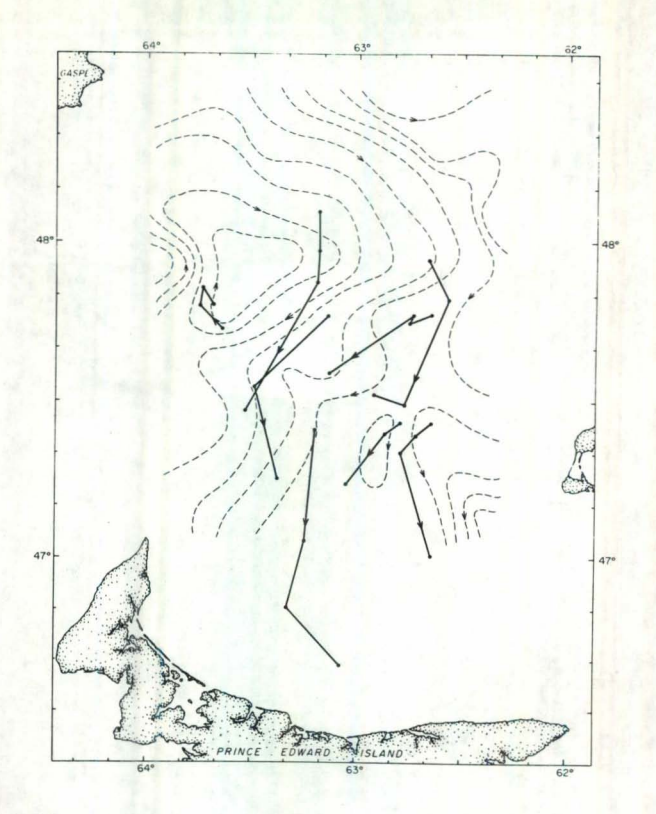


Fig. 11. Tracks of subsurface bubys superimposed on Phase 1 geopotential anomalies, Cruise 3368.

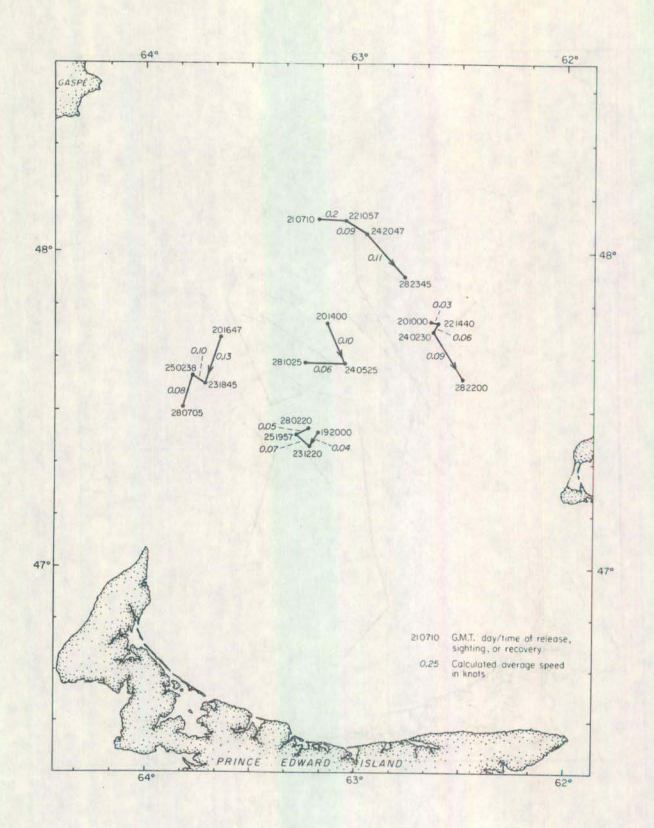


Fig. 12. Tracks of 40-metre parachute drogues, and calculated average speeds between sightings. Cruise 3368.

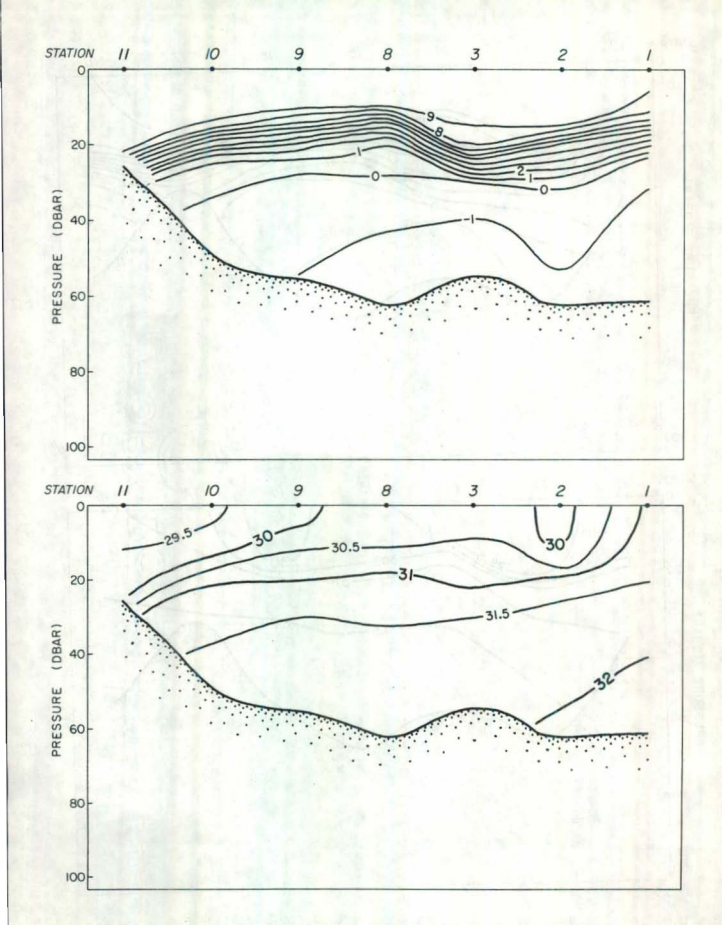


Fig. 13. Temperature (top) and salinities (bottom) cross-section, Row 9, Cruise 3368, Phase 1.

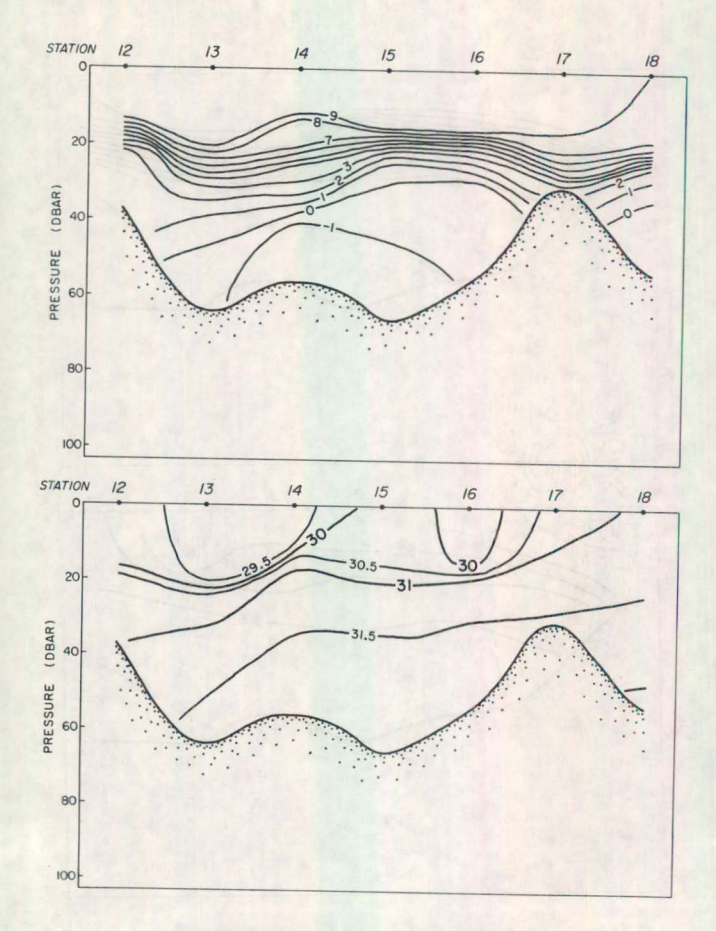


Fig. 14. Temperature (top) and salinity (bottom) cross-section, Row 8, Cruise 3368, Phase 1.

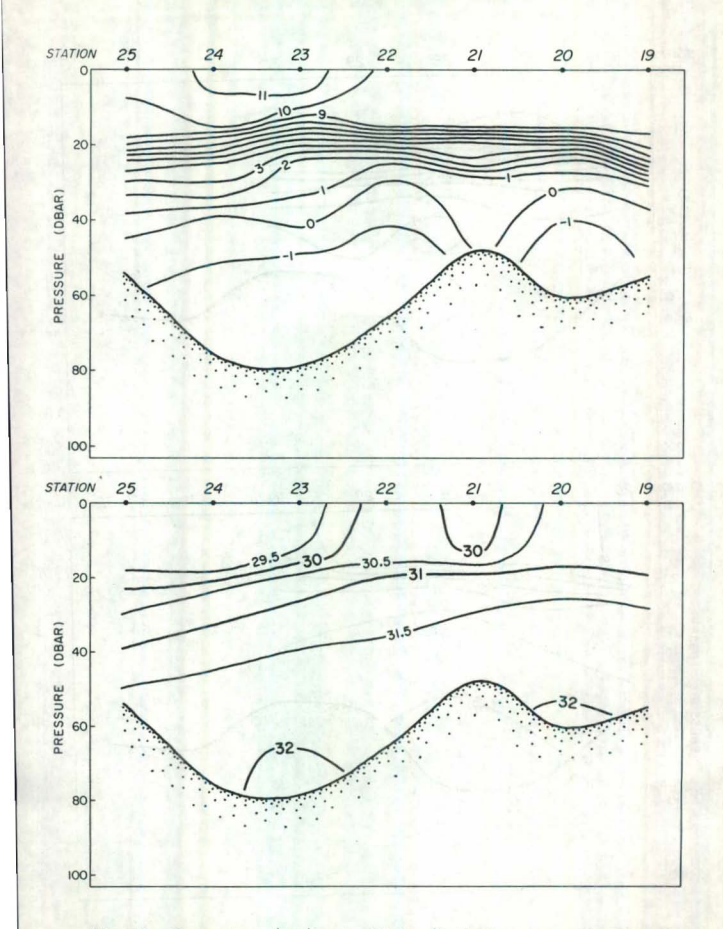


Fig. 15. Temperature (top) and salinity (bottom) cross-section, Row 7, Cruise 3368, Phase 1.

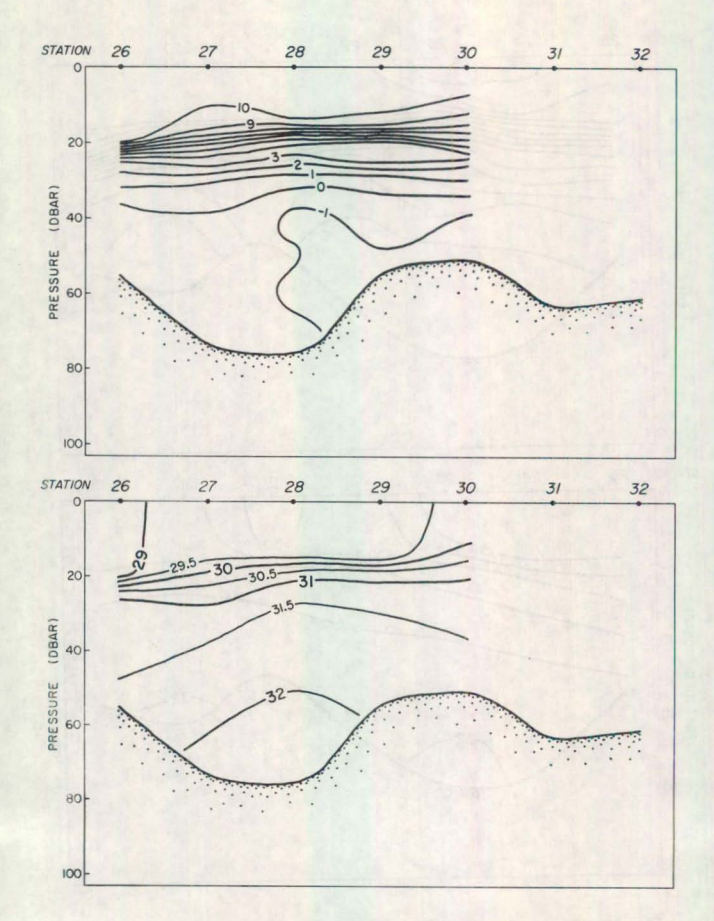


Fig. 16. Temperature (top) and salinity (bottom) cross-section, Row 6, Cruise 3368, Phase 1.

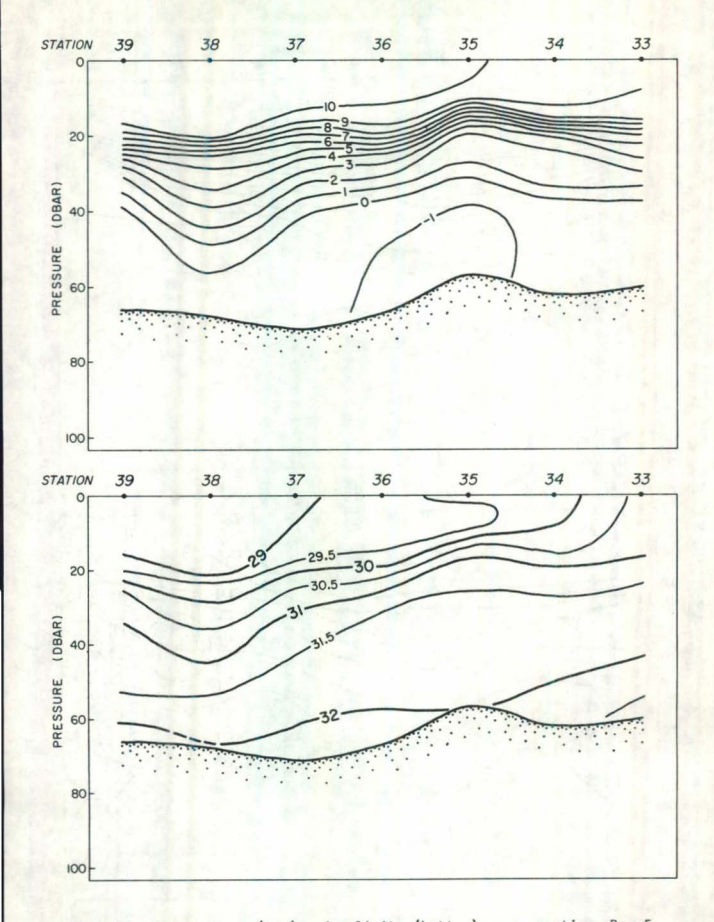


Fig. 17. Temperature (top) and salinity (bottom) cross-section, Row 5,

Cruise 3368, Phase 1.

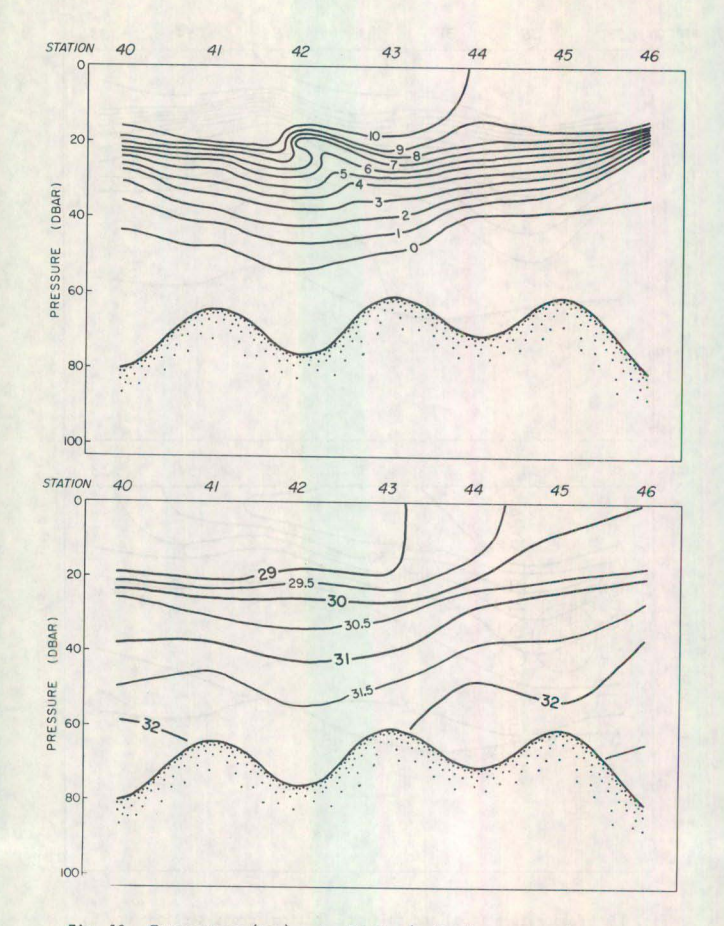


Fig. 18. Temperature (top) and salinity (bottom) cross-section, Row 4, Cruise 3368, Phase 1.

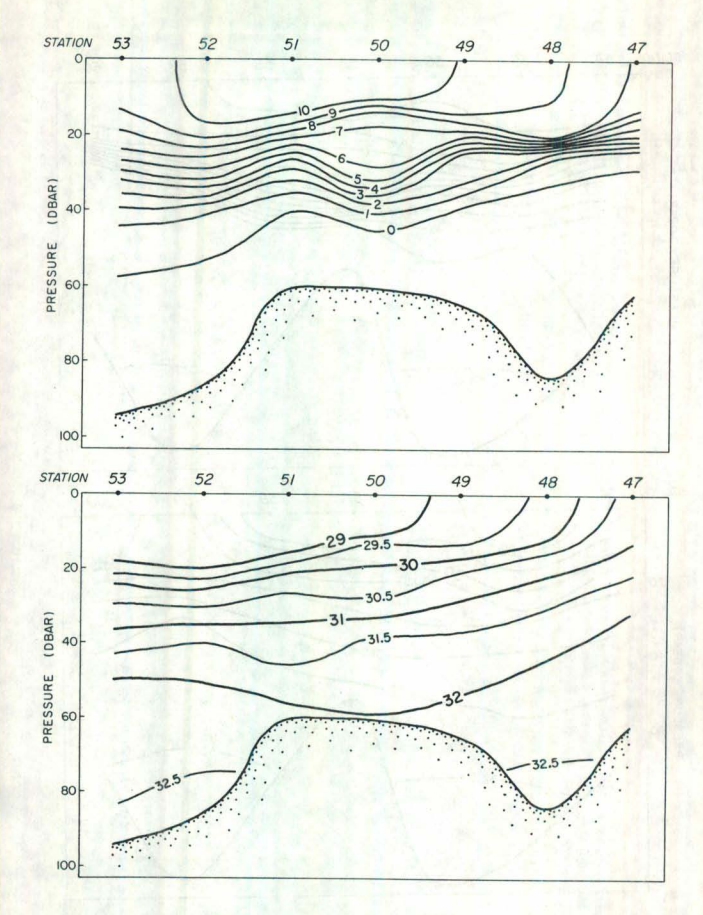


Fig. 19. Temperature (top) and salinity (bottom) cross-section, Row 3, Cruise 3368, Phase 1.

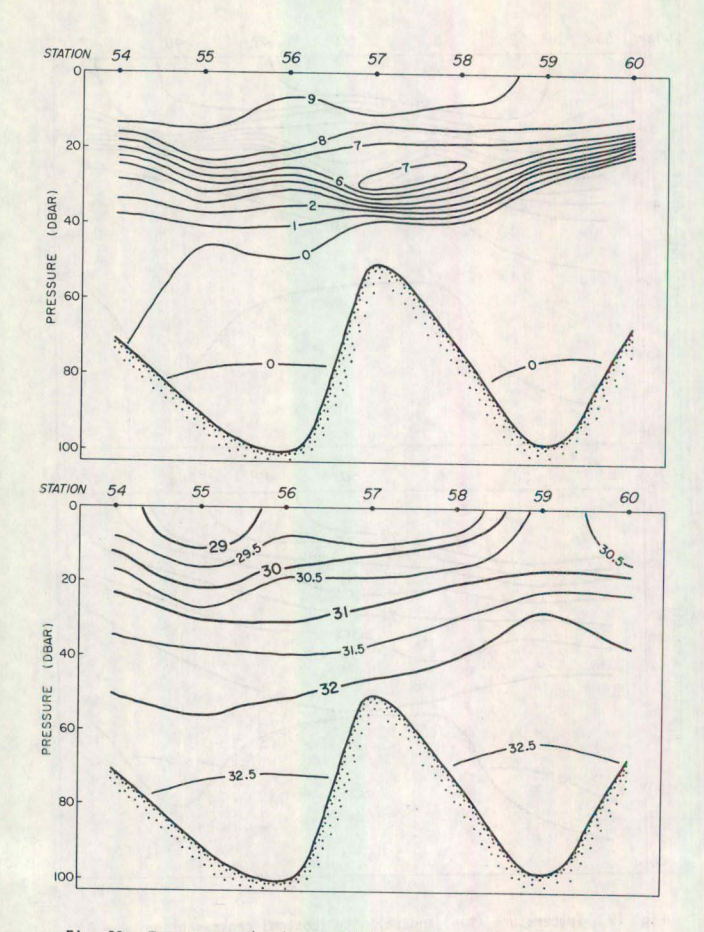


Fig. 20. Temperature (top) and salinity (bottom) cross-section, Row 2, Cruise 3368, Phase 1.

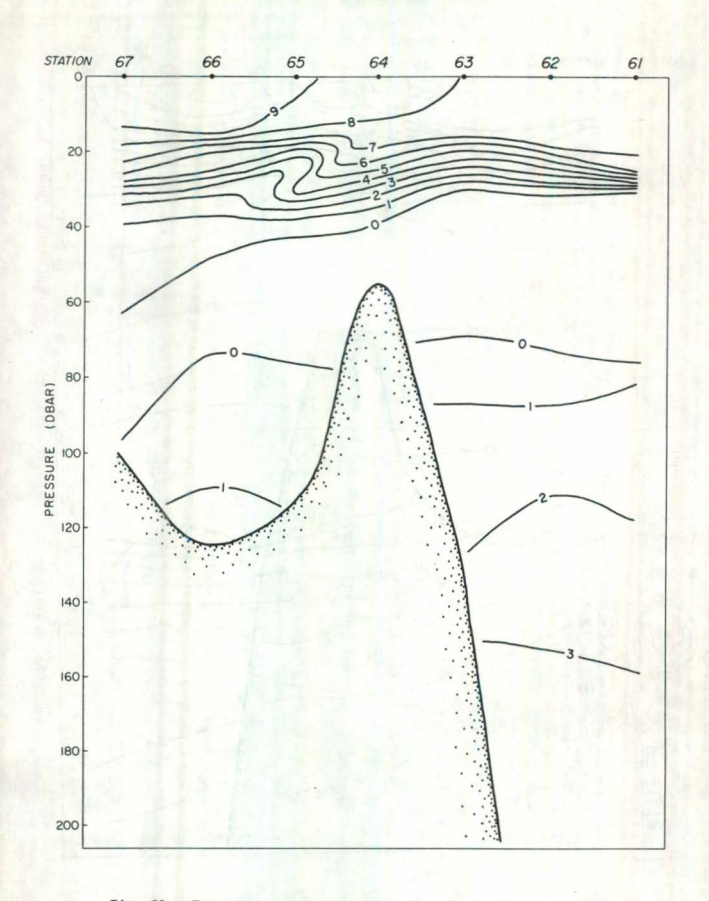


Fig. 21. Temperature cross-section, Row 1, Cruise 3368, Phase 1

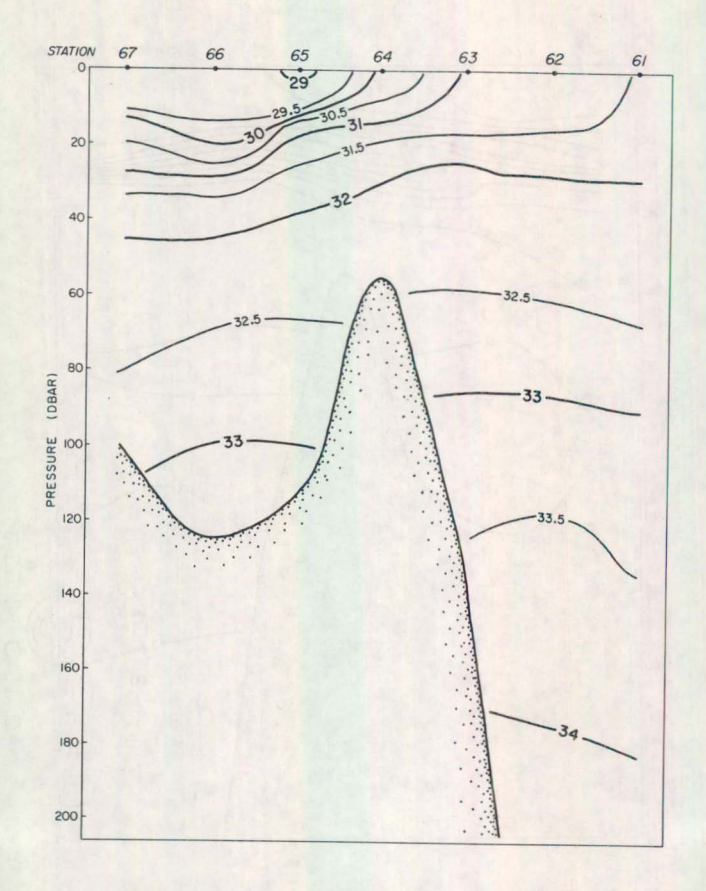


Fig. 22. Salinity cross-section, Row 1, Cruise 3368, Phase 1.

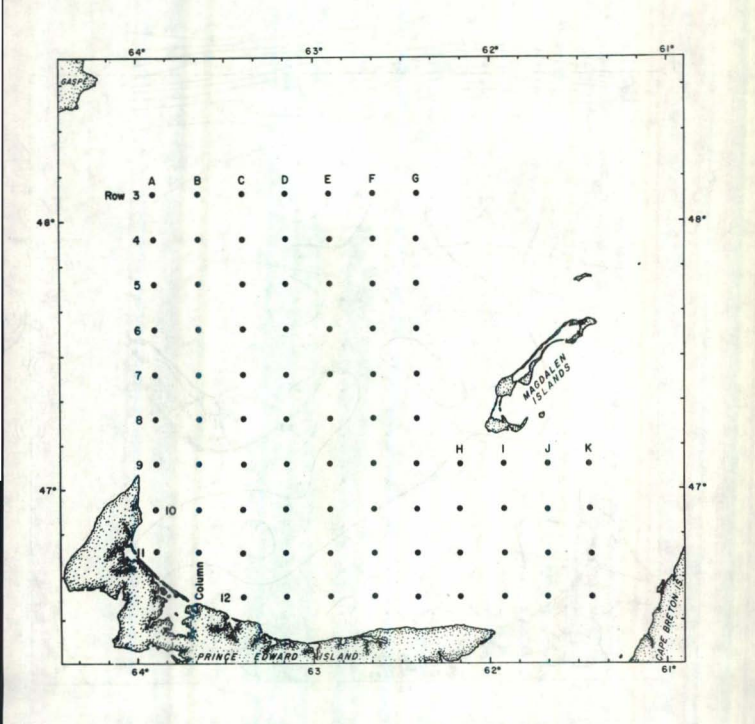


Fig. 23. Phase 2 of Cruise 3368. See Table 2, Stations 76-172

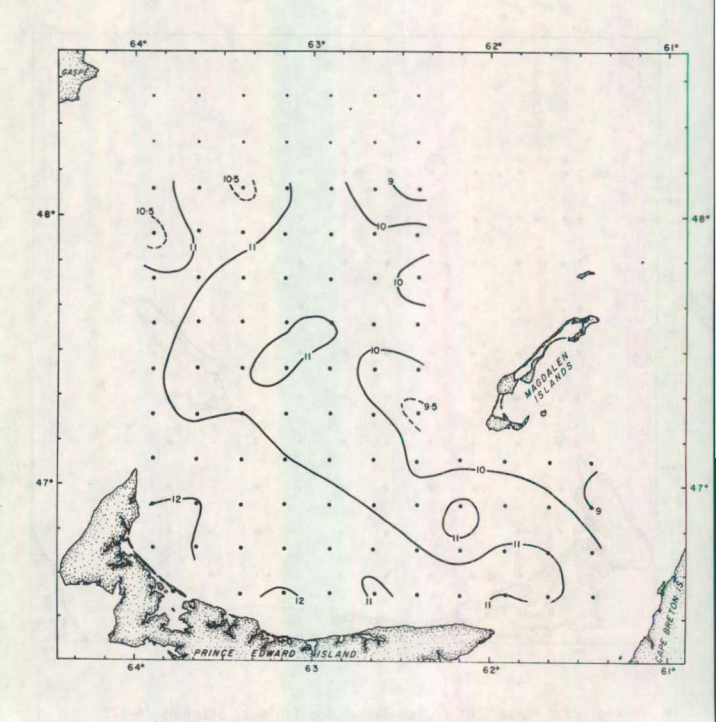


Fig. 24. Surface temperatures, Cruise 3368, Phase 2

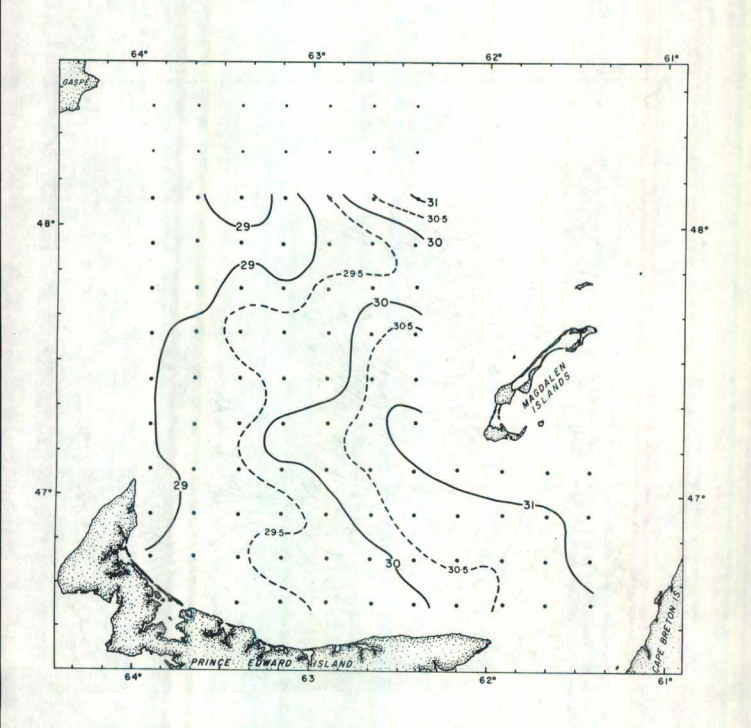


Fig. 25. Surface salinities, Cruise 3368, Phase 2

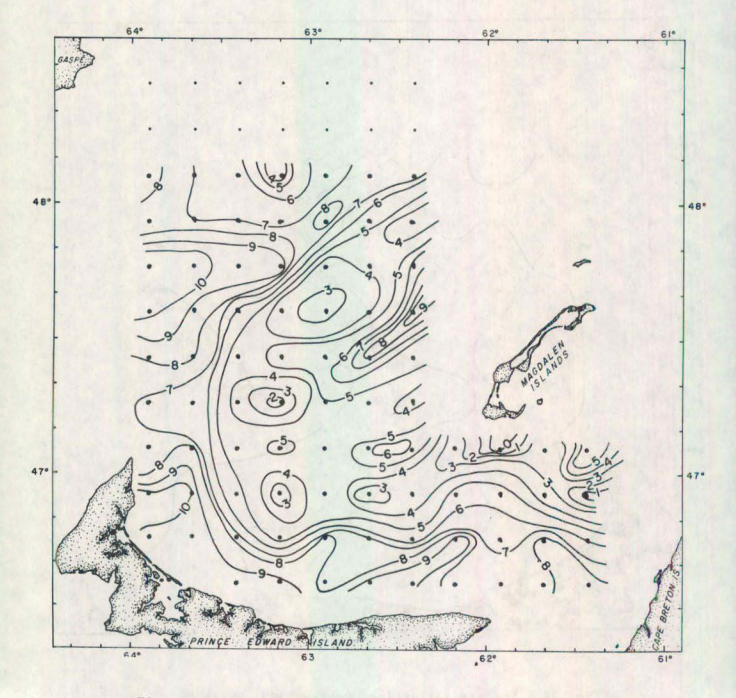


Fig. 26. 20 dbar temperatures, Cruise 3368, Phase 2

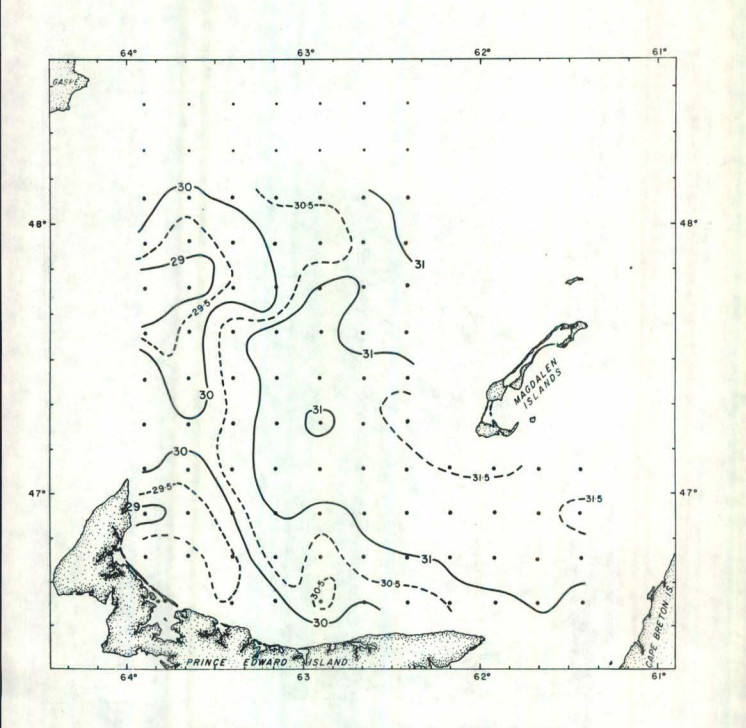


Fig. 27. 20 dbar salinities, Cruise 3368, Phase 2

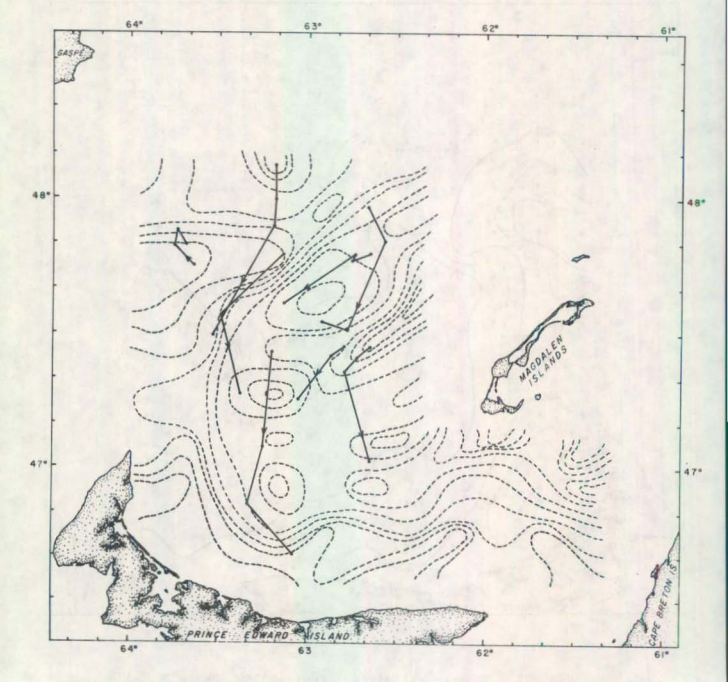


Fig. 28. Tracks of subsurface dorgues superimposed on Phase 2 20-dbar isotherms Cruise 3368.

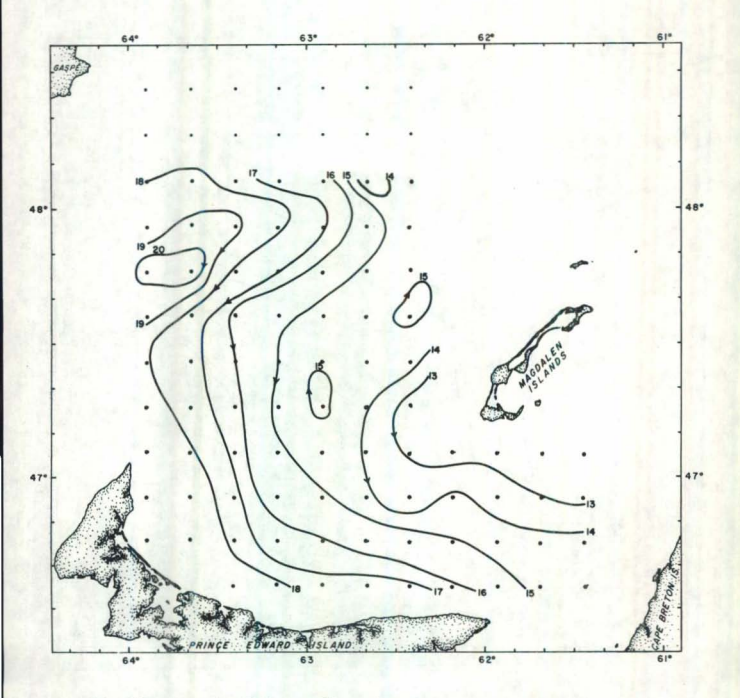


Fig. 29. Geopotential anomalies, dynamic centimetres relative to 40 dbar Cruise 3368, Phase 2

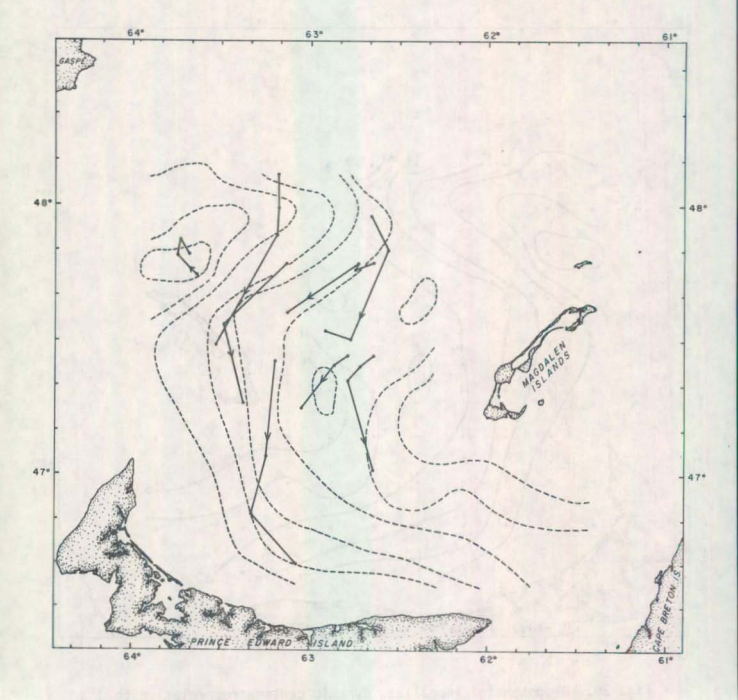


Fig. 30. Tracks of subsurface buoys superimposed on geopotential anomalies Cruise 3368, Phase 2

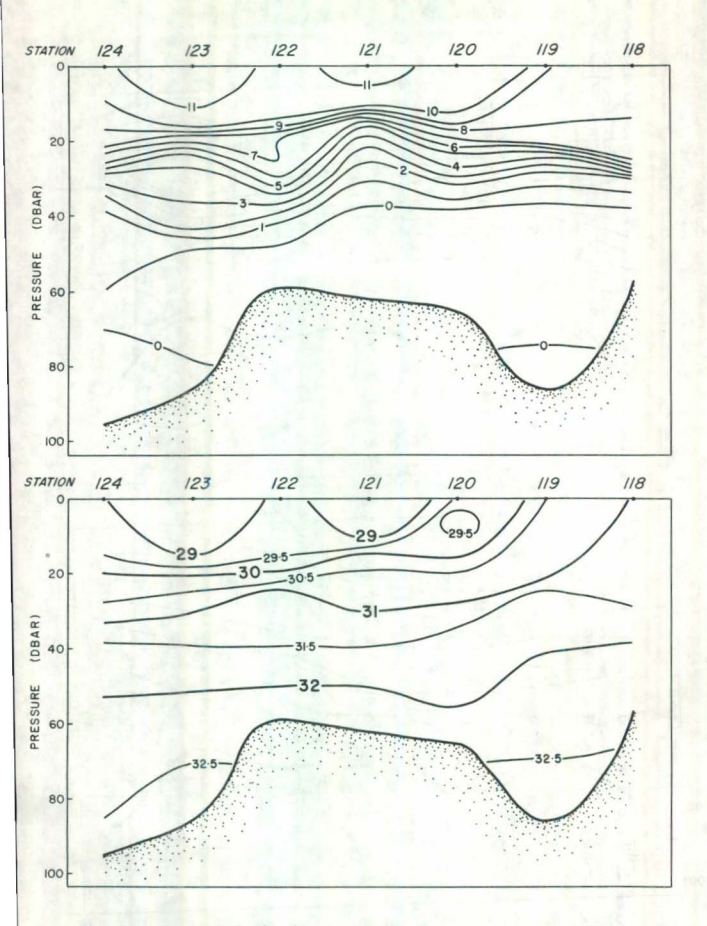


Fig. 31. Temperature (top) and salinity (bottom) cross-section, Row 3,
Cruise 3368, Phase 2

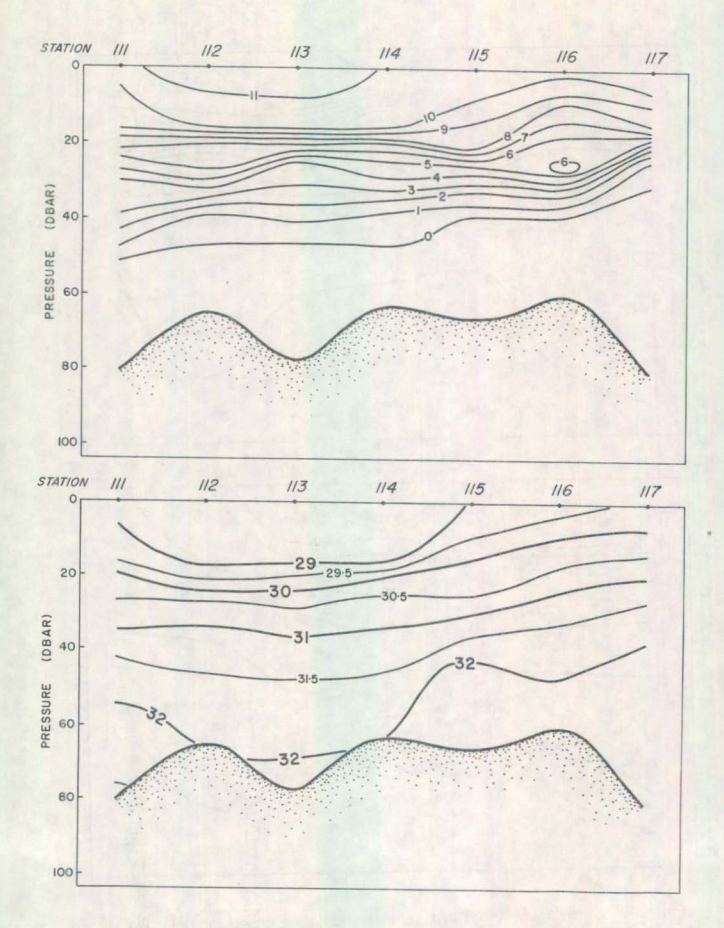


Fig. 32. Temperature (top) and salinity (bottom) cross-section, Row 4, Cruise 3368, Phase 2

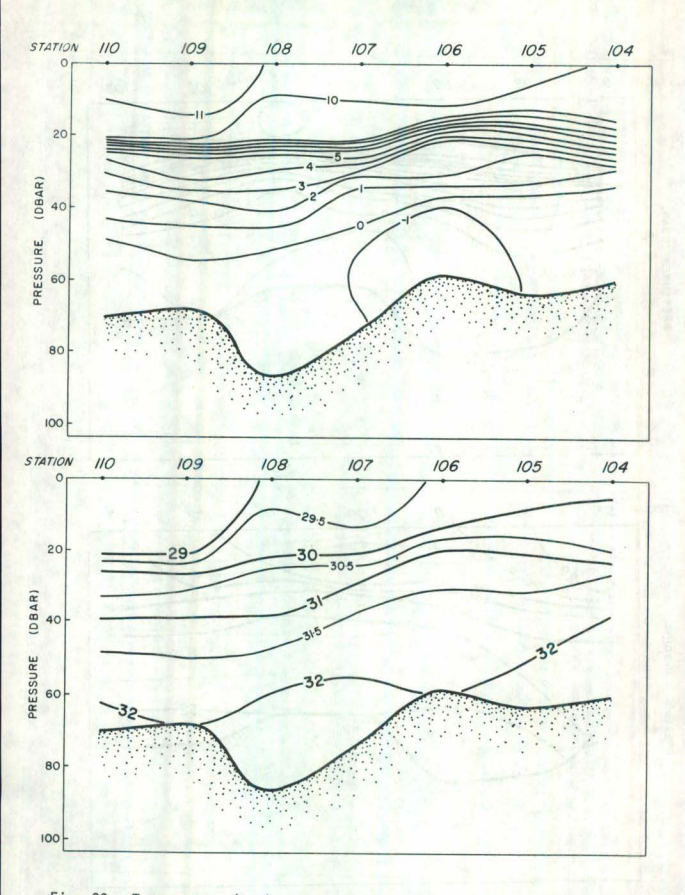


Fig. 33. Temperature (top) and salinity (bottom) cross-section, Row 5,
Cruise 3368, Phase 2

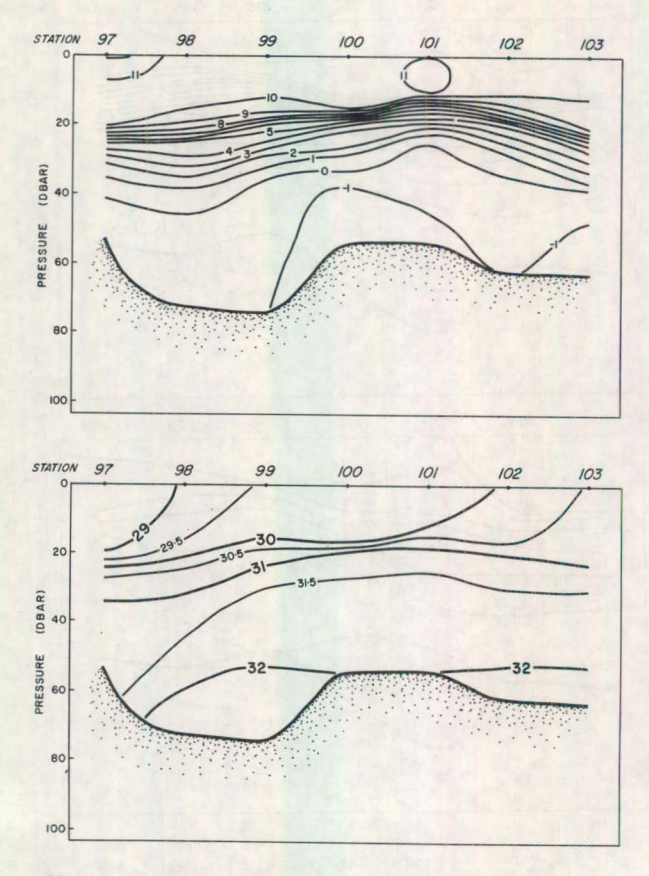


Fig. 34. Temperature (top) and salinity (bottom) cross-section, Row 6, Cruise 3368, Phase 2.

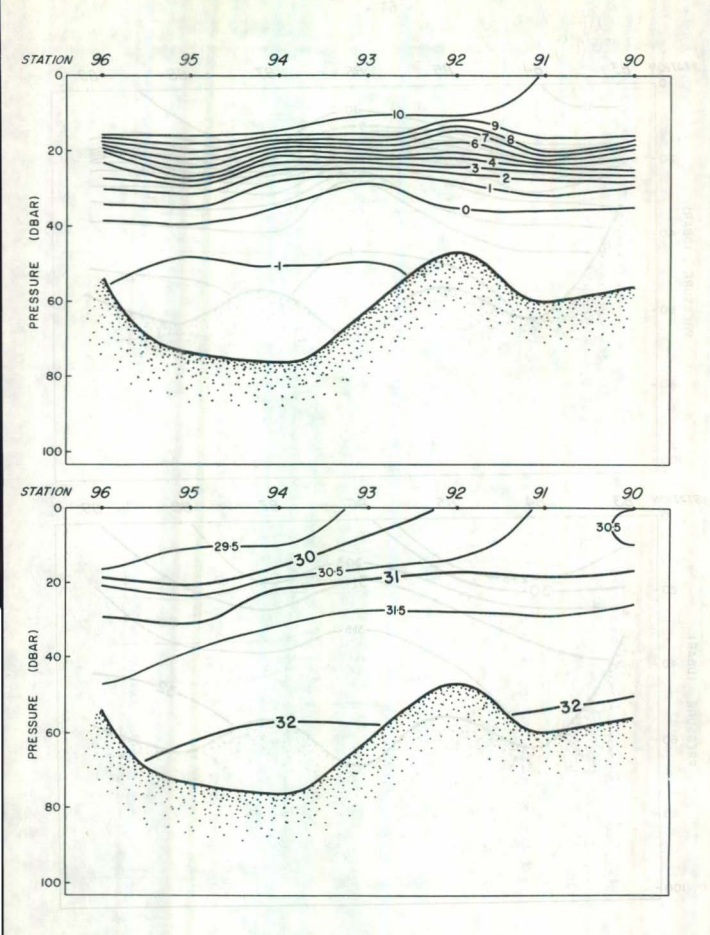


Fig. 35. Temperature (top) and salinity (bottom) cross-section, Row 7, Proceedings and Salinity (bottom) cross-section, Row 7, Proceedings and Company (Salinity Company) and Salinity (bottom) cross-section, Row 7, Proceedings and Salinity (bottom) cross-section (bottom) cross-

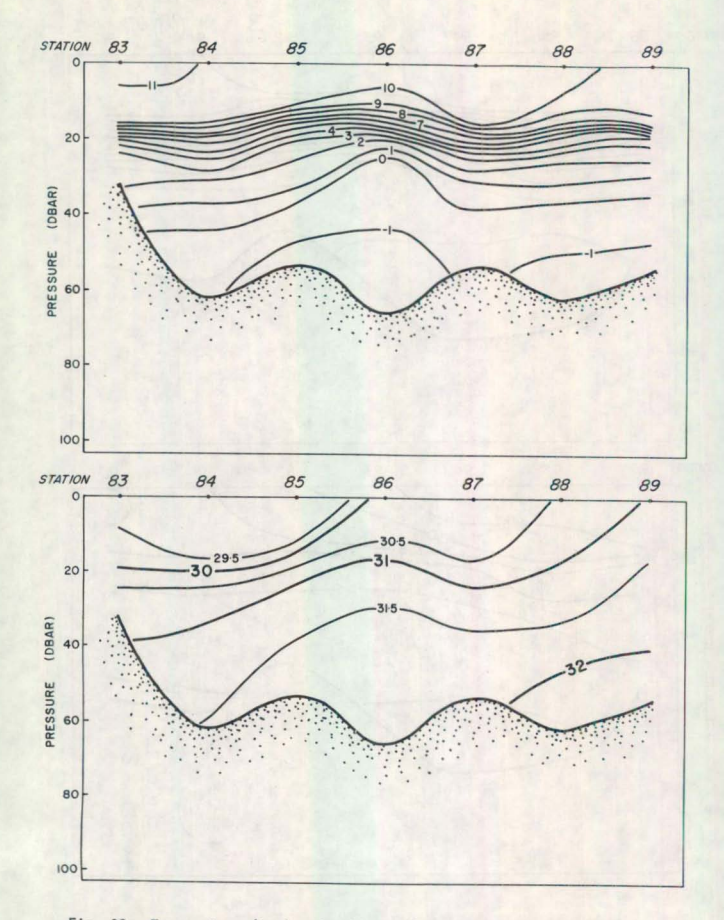


Fig. 36. Temperature (top) and salinity (bottom) cross-section, Row 8, Cruise 3368, Phase 2.

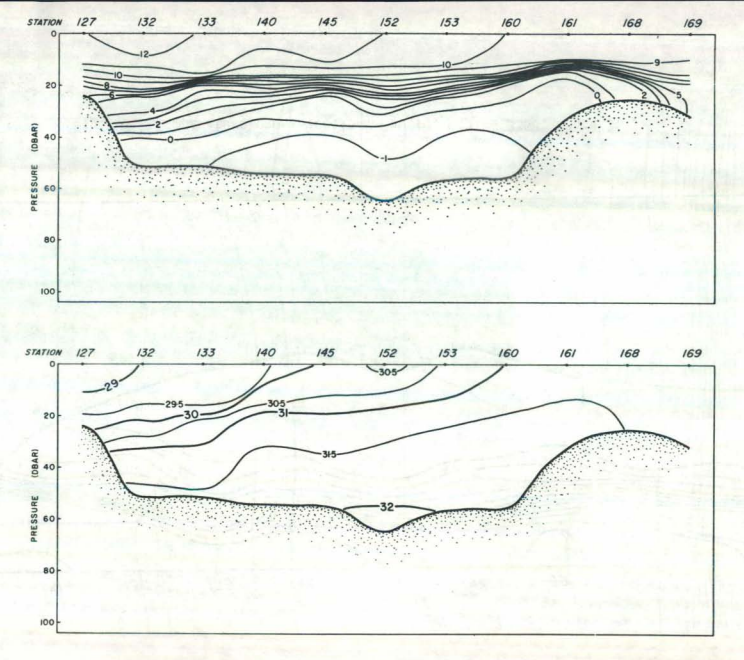


Fig. 37. Temperature (top) and salinity (bottom) cross-section, Row 9, Cruise 3368, Phase 2.

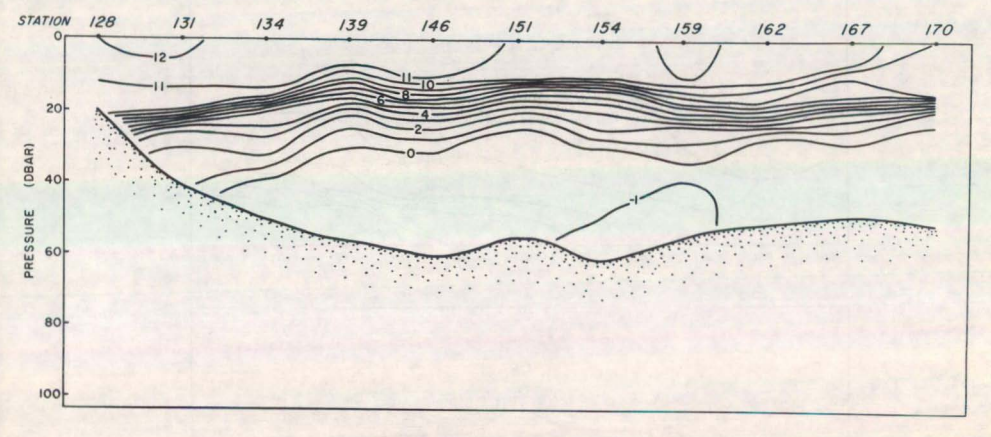


Fig. 38. Temperature cross-section, Row 10, Cruise 3368, Phase 2.

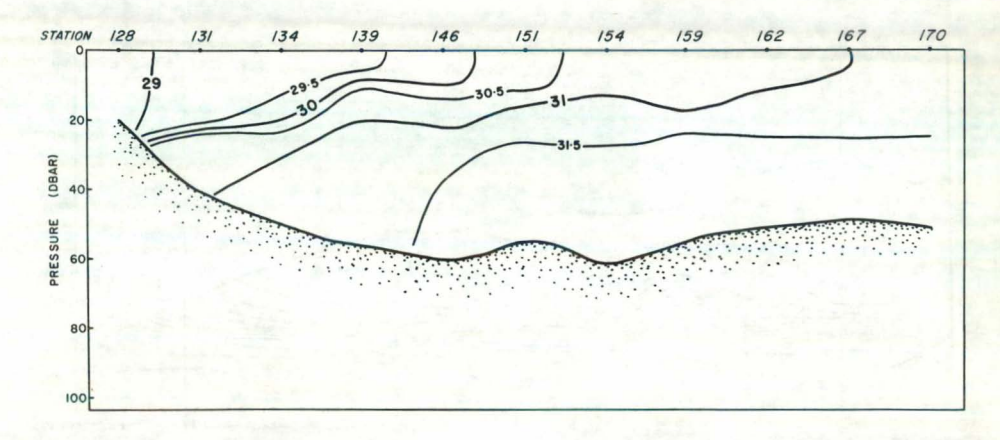


Fig. 39. Salinity cross-section, Row 10, Cruise 3368, Phase 2.

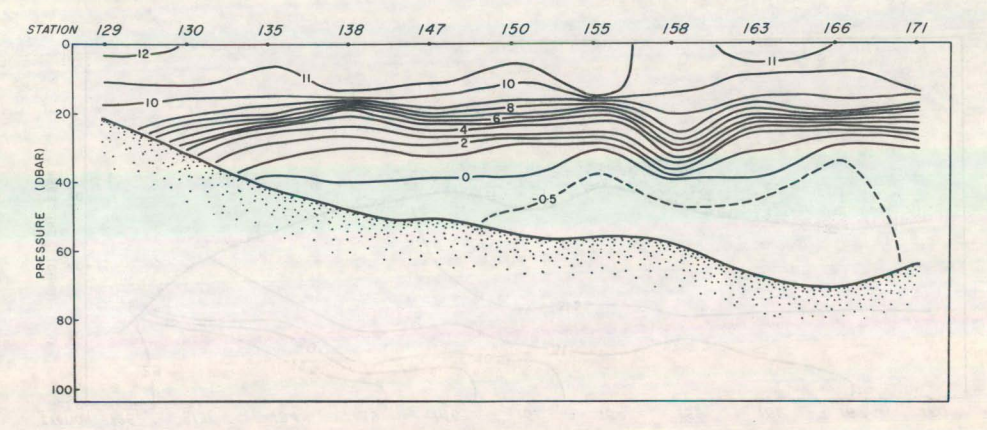


Fig. 40. Temperature cross-section, Row 11, Cruise 3368, Phase 2.

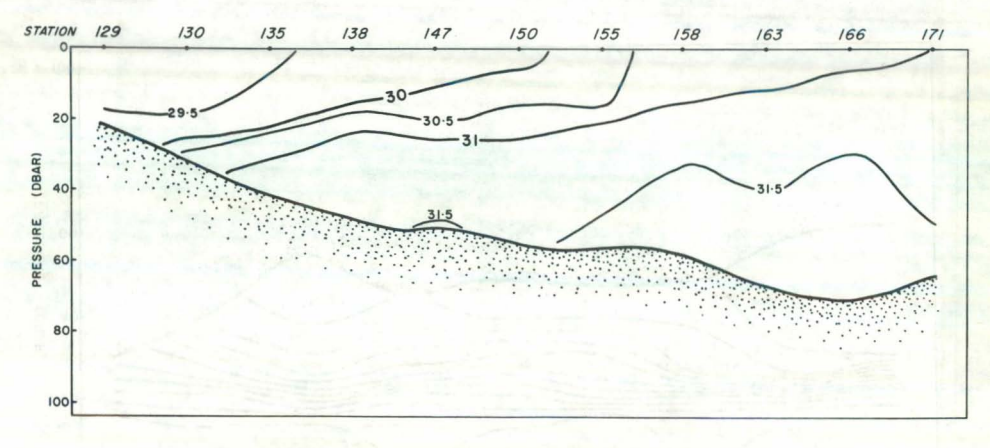


Fig. 41. Salinity cross-section, Row 11, Cruise 3368, Phase 2.

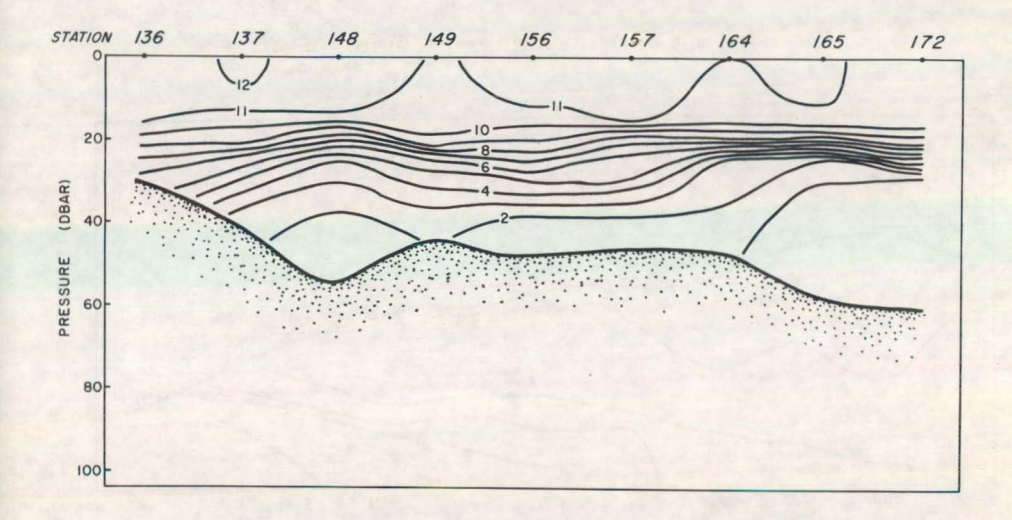


Fig. 42. Temperature cross-section, Row 12, Cruise 3368, Phase 2.

Fig. 43. Salinity cross-section, Row 12, Cruise 3368, Phase 2

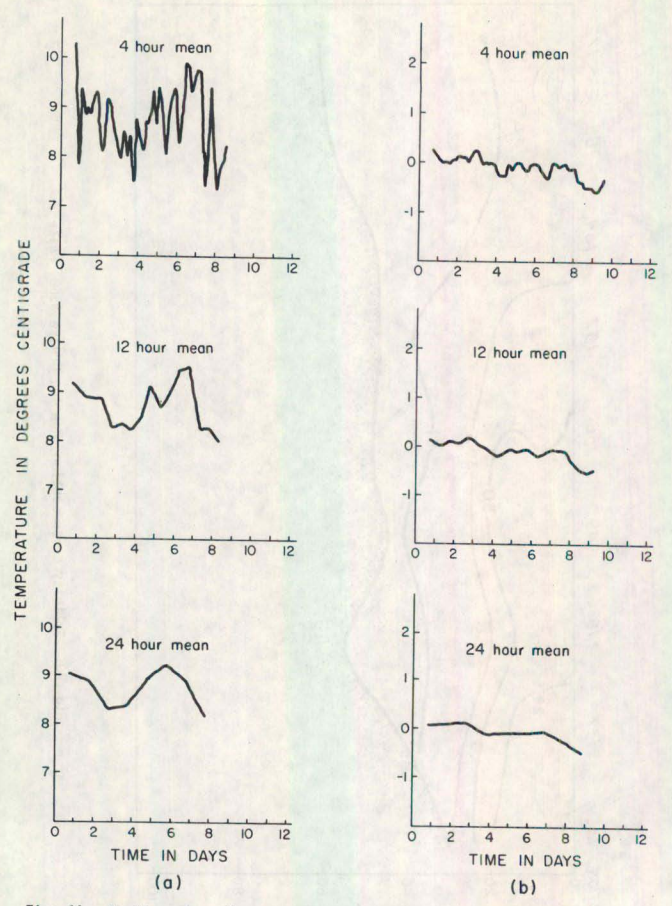
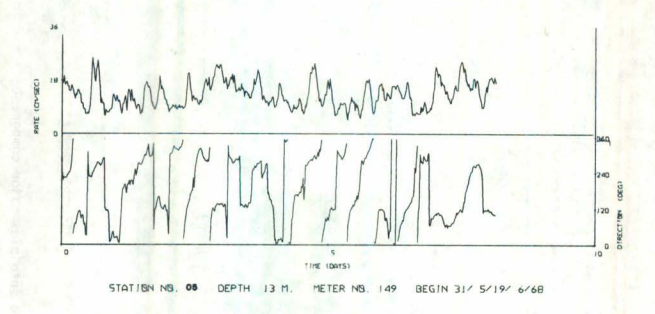


Fig. 44. Readings from thermographs submerged at (a) 12m and (b) 45m, at grid position 7E, Bradelle Bank, Cruise 3368. Twenty-minute readings have been here averaged over 4-hour, 12-hour, and 24-hour periods. Starting date 18/6/68. See Tables 3 and 4.



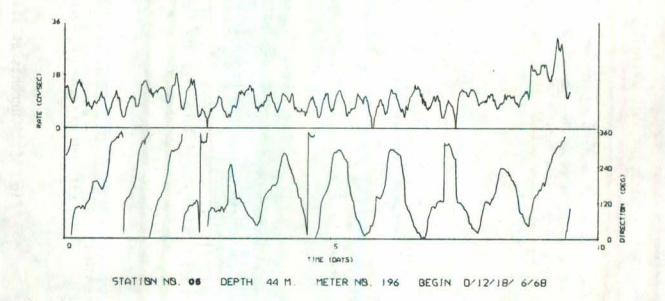
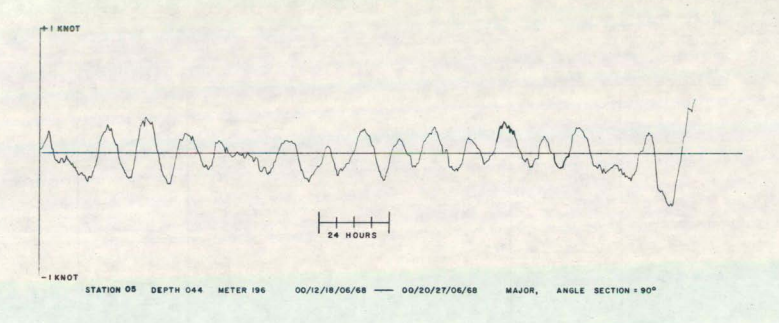


Fig. 45. Currents (rate and true direction)at 13m (top)and 44m (bottom), Cruise 3368. Mooring lay was completed at 2140Z on 18/6/68; mooring recovery was completed at 1330Z on 28/6/68. See text.



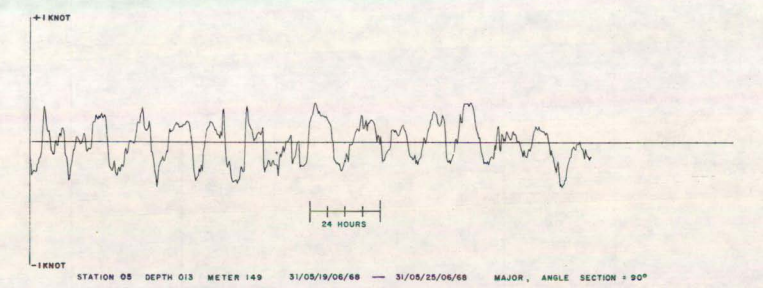


Fig. 46. Currents at station 5, resolved into plus major component North, minus major component South. Cruise 3368.

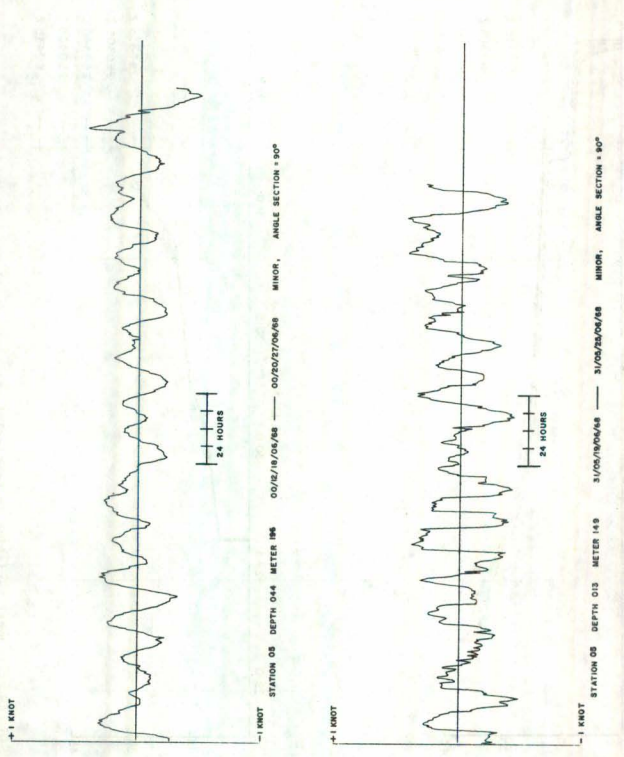
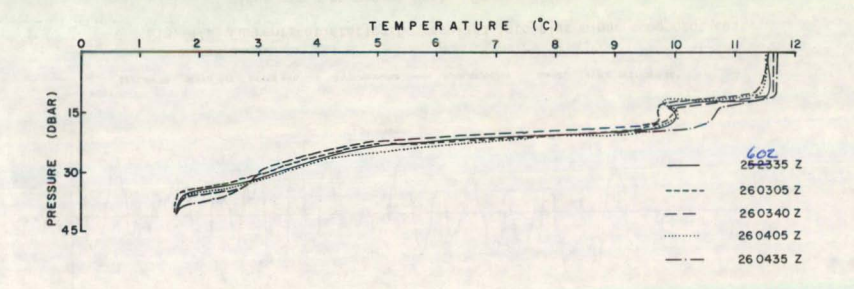


Fig. 47. Currents at station 5, resolved into plus minor component East, minus minor component West. Cruise 3368.





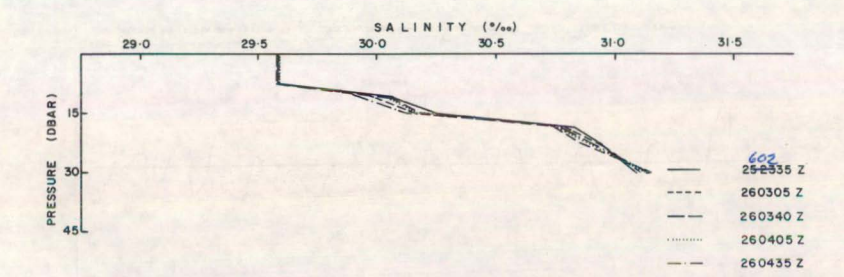


Fig. 48. Temporal variation in vertical temperature (top) and salinity (bottom) readings, Station 148 grid position 12E, Cruise 3368, Phase 2

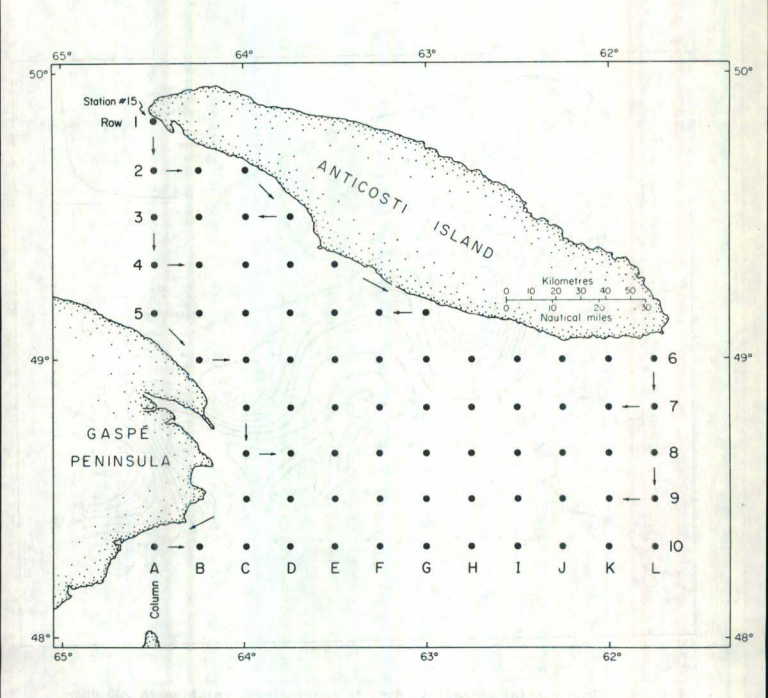


Fig. 49. Location of grid points for Cruise 69-051, June 23-27, 1969.

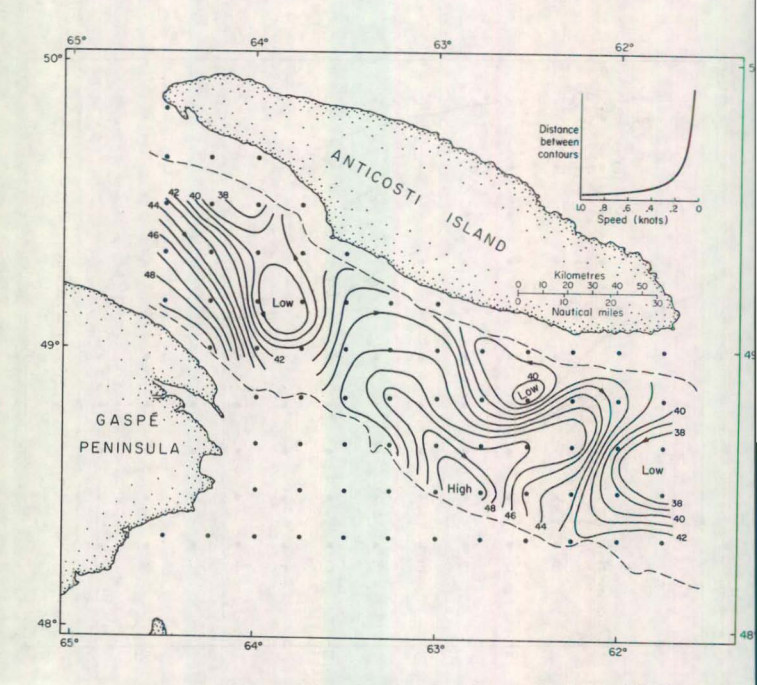


Fig. 50. Geopotential anomalies, dynamic centimetres, relative to 200 dbar, Cruise 69-051

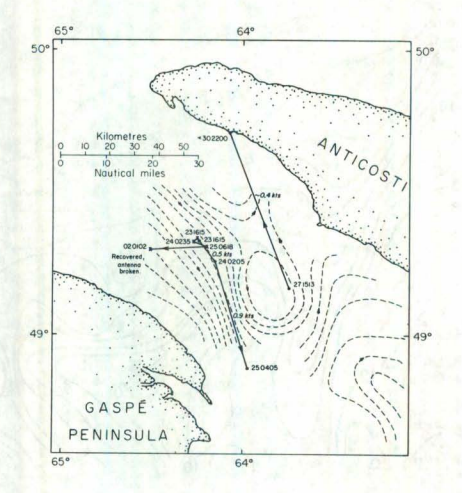


Fig. 51. Movement of two subsurface (10m) drogues and one 40m drogue (recovered, antenna broken) superimposed on geopotential anomalies relative to 200 dbar. (For explanation of numbers, see Fig. 8). DAWSON reached south coast of Anticosti Island at 2200 GMT on Sept. 30 but beached drogue could not be recovered. Cruise 69-051.

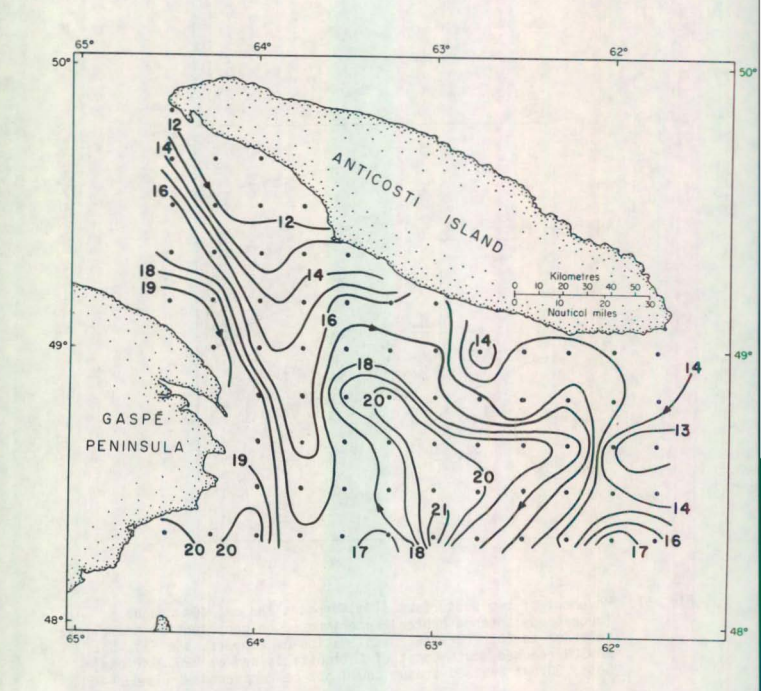


Fig. 52. Geopotential anomalies, dynamic centimetres, relative to 40 dbar. Cruise 69-051.

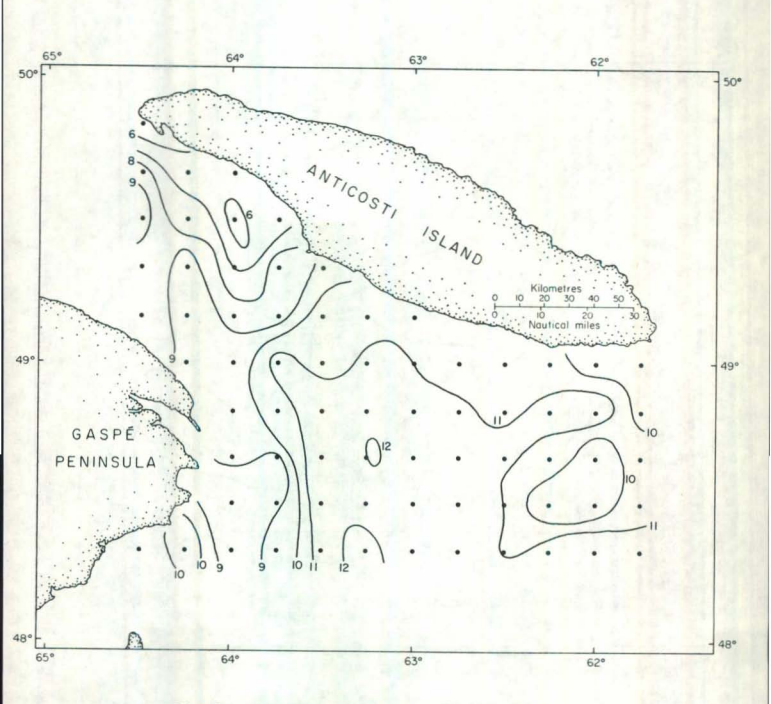


Fig. 53. Surface temperatures, Cruise 69-051.

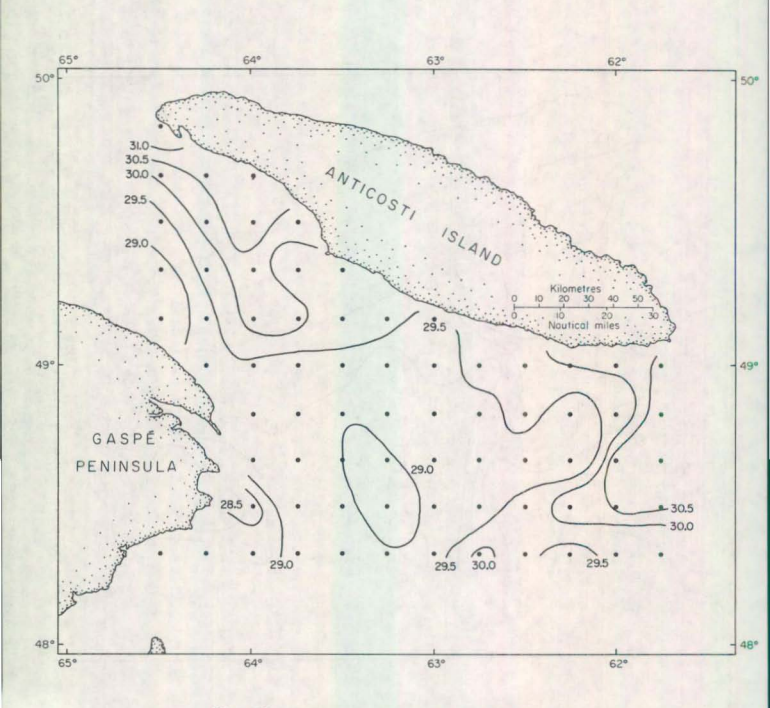


Fig. 54. Surface salinities, Cruise 69-051.

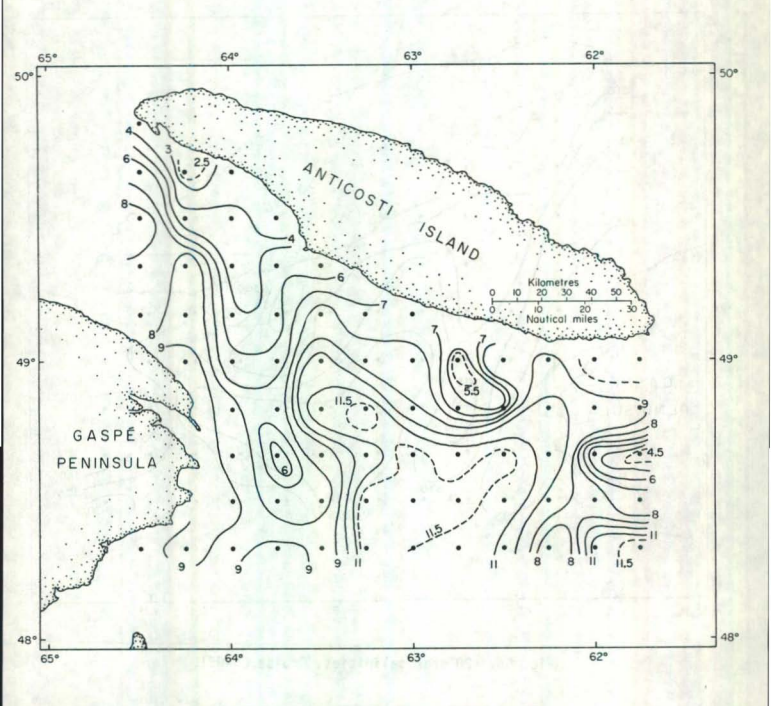


Fig. 55. 20 dbar temperatures, Cruise 69-051.

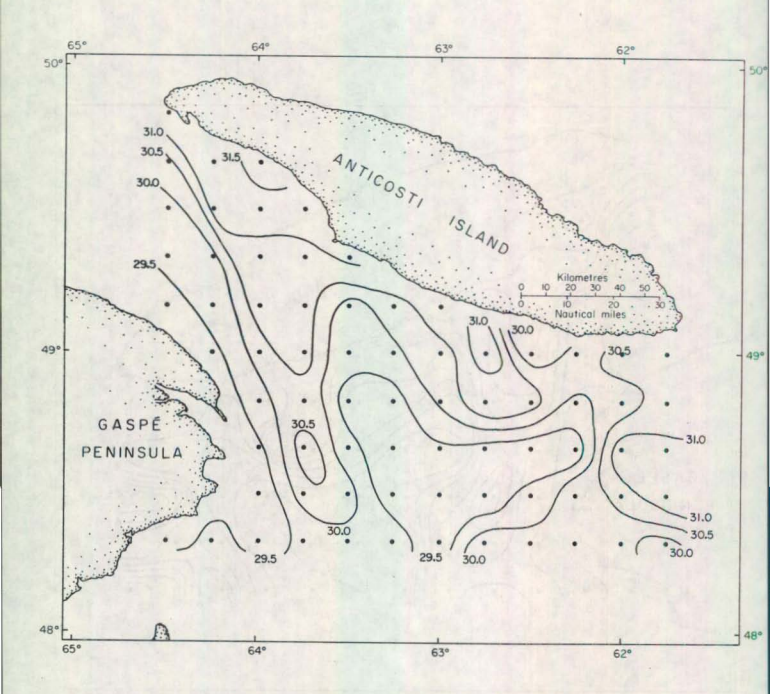


Fig. 56. 20 dbar salinities, Cruise 69-051.

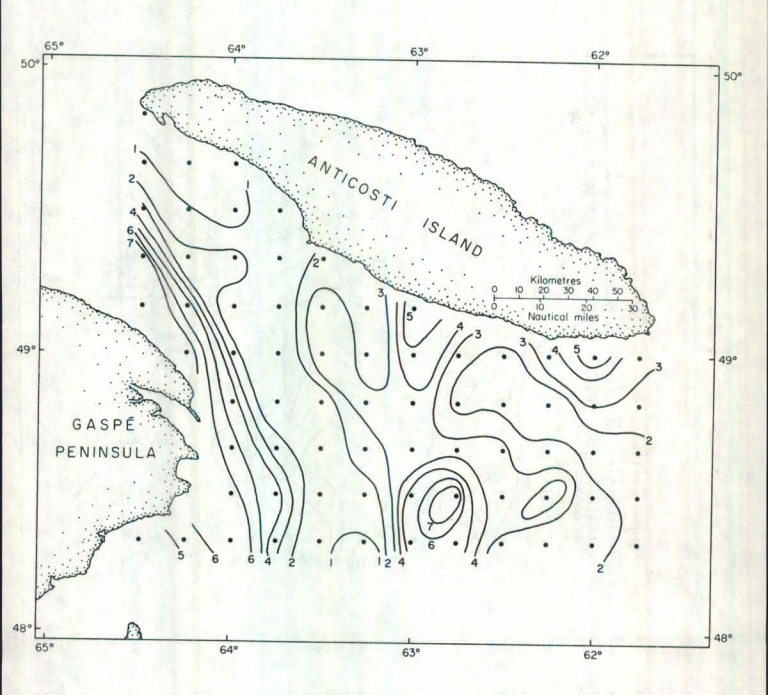


Fig. 57. 40 dbar temperatures, Cruise 69-051.

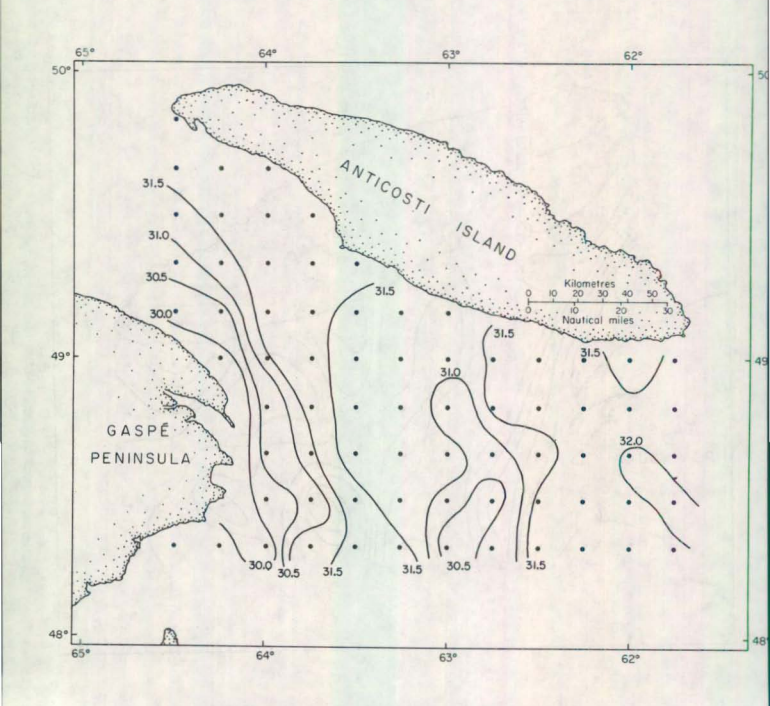


Fig. 58. 40 dbar salinities, Cruise 69-051.

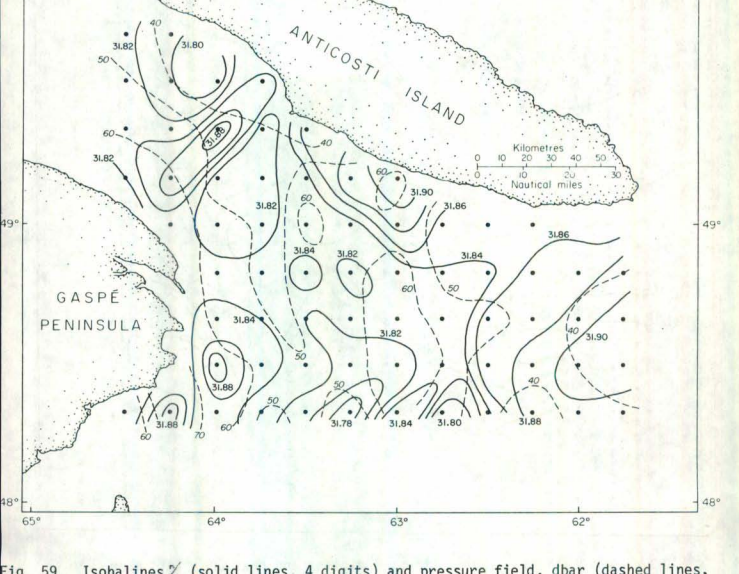


Fig. 59. Isohalines % (solid lines, 4 digits) and pressure field, dbar (dashed lines, italic digits) on σ_0 = 25.5 surface, Cruise 69-051.

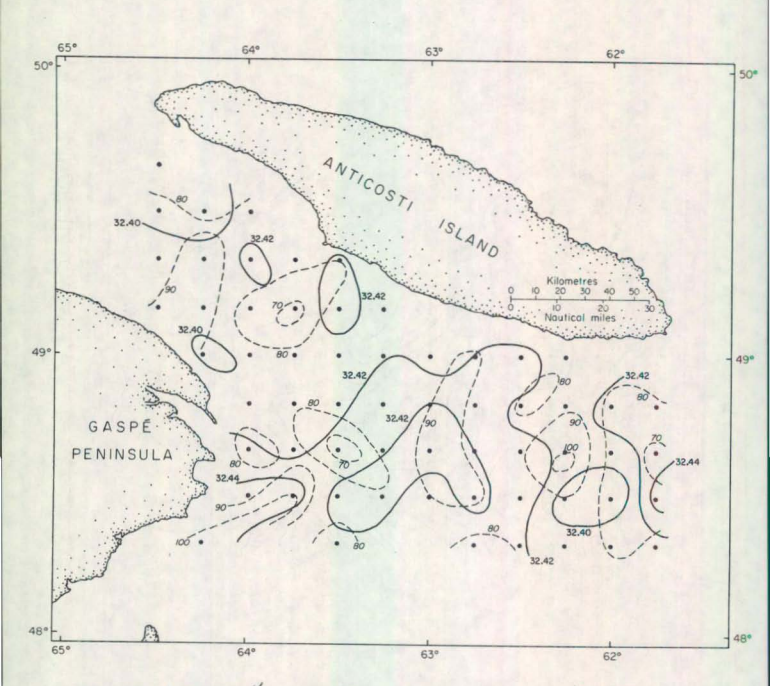


Fig. 60. Isohalines % (solid lines, 4 digits) and pressure field dbar (dashed lines, italic digits), on σ_{\odot} = 26.0 surface, Cruise 69-051.

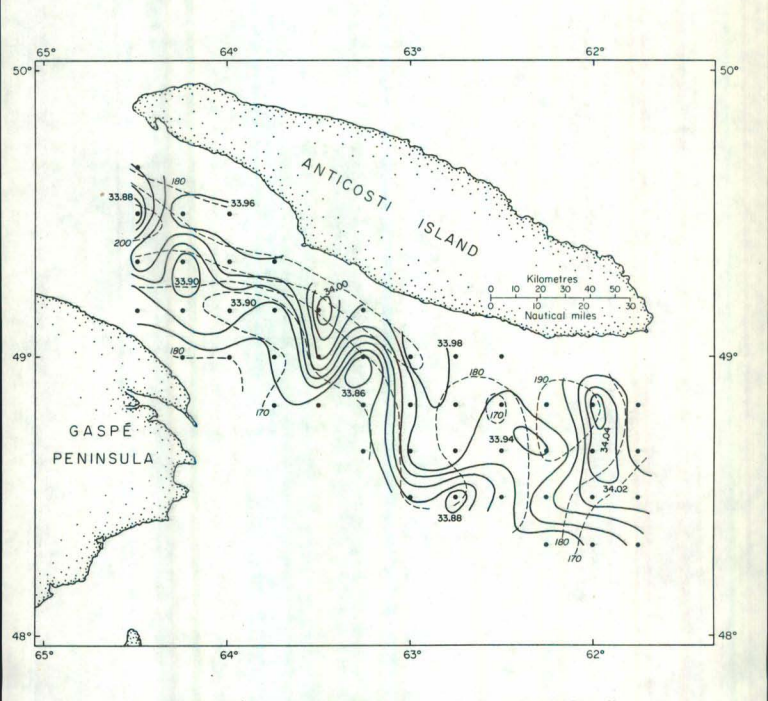


Fig. 61. Isohalines%(solid lines, 4 digits) and pressure field, dbar (dashed lines, italic digits) on σ_0 = 27.0 surface, Cruise 69-051.

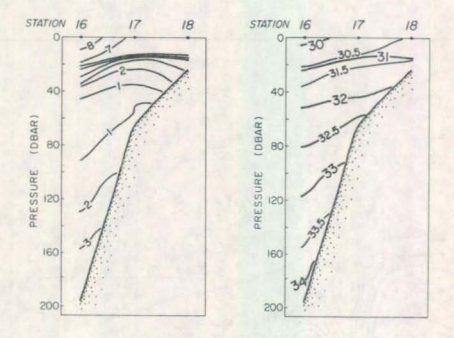


Fig. 62. Temperature (left) and salinity (right) cross-section of Row 2, Cruise 69-051.

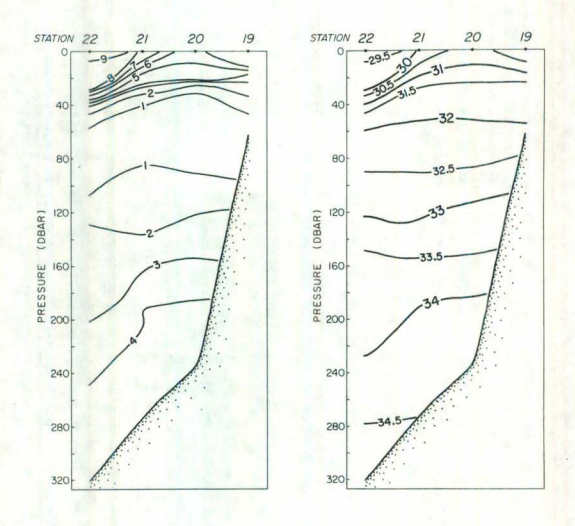


Fig. 63. Temperature (left) and salinity (right) cross-section of Row 3, Cruise 69-051.

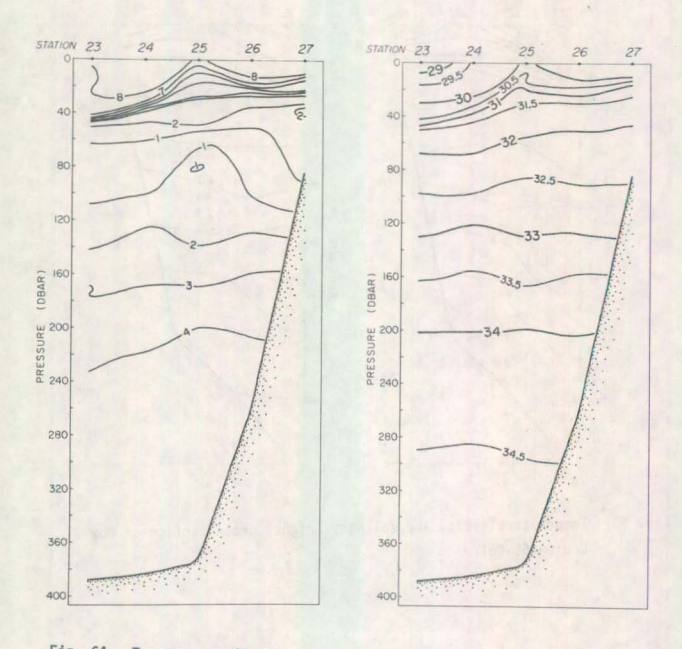


Fig. 64. Temperature (left) and salinity (right) cross-section of Row 4, Cruise 69-051.

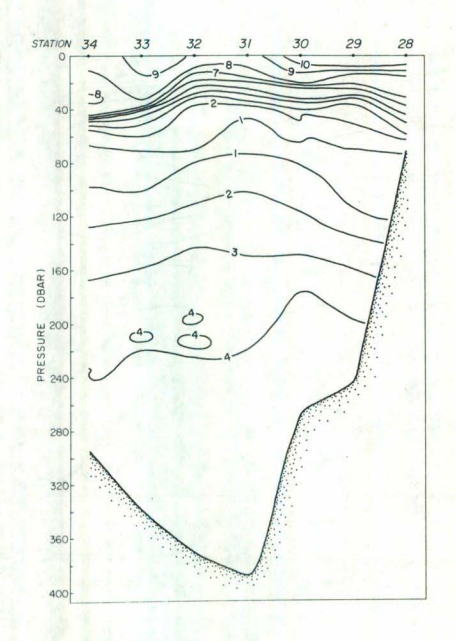


Fig. 65. Temperature cross-section Row 5, Cruise 69-051.

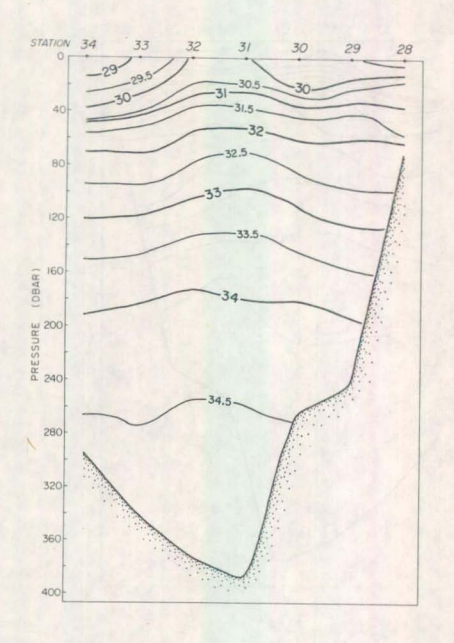


Fig. 66. Salinity cross-section, Row 5, Cruise 69-051.

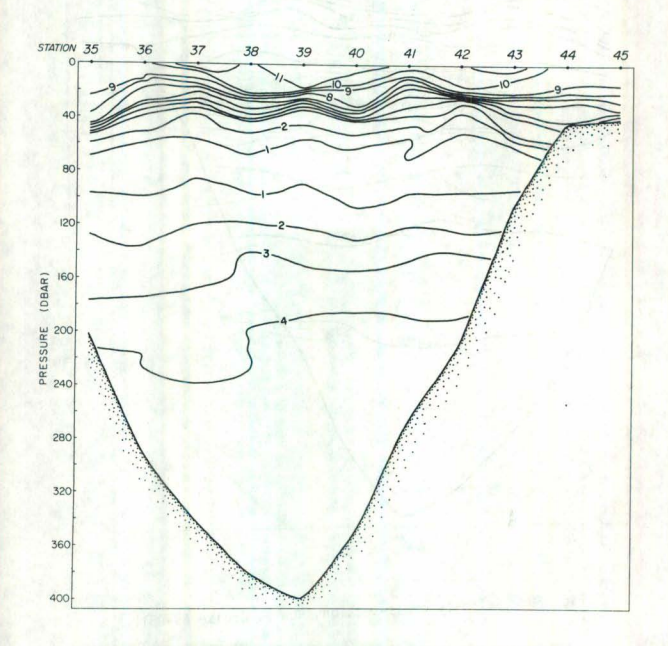


Fig. 67. Temperature cross-section, Row 6, Cruise 69-051.

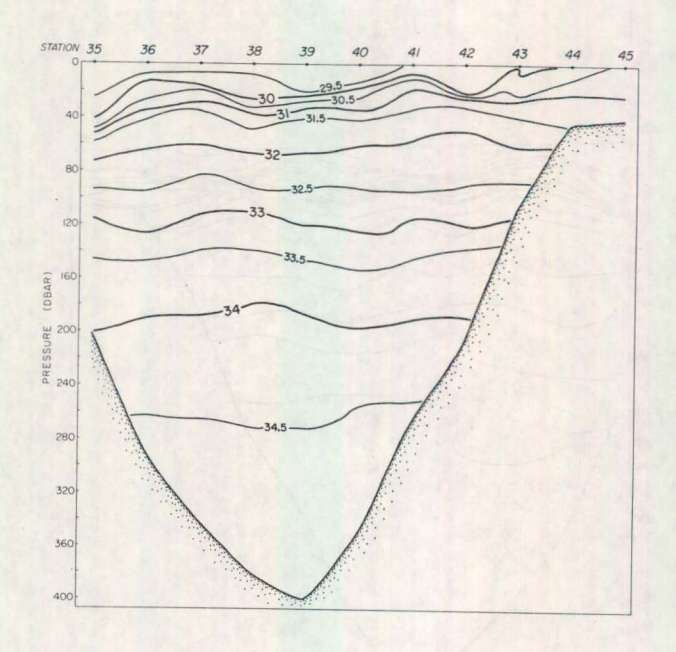


Fig. 68. Salinity cross-section, Row 6, Cruise 69-051.

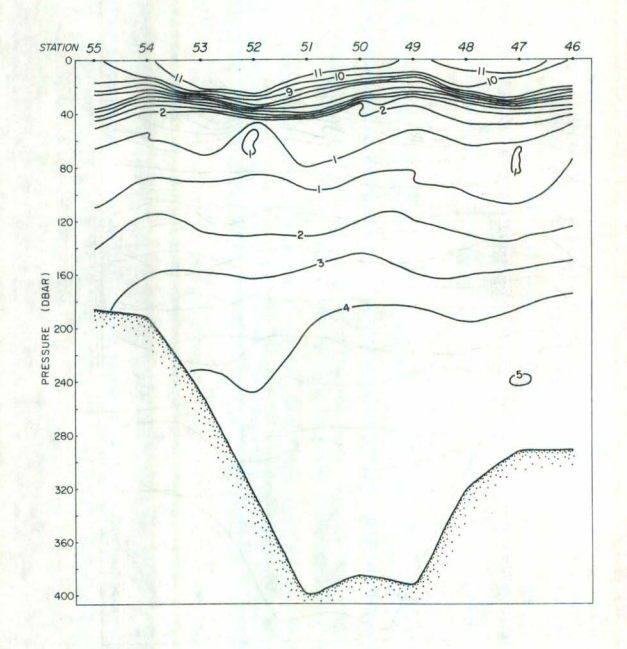


Fig. 69. Temperature cross-section, Row 7, Cruise 69-051.

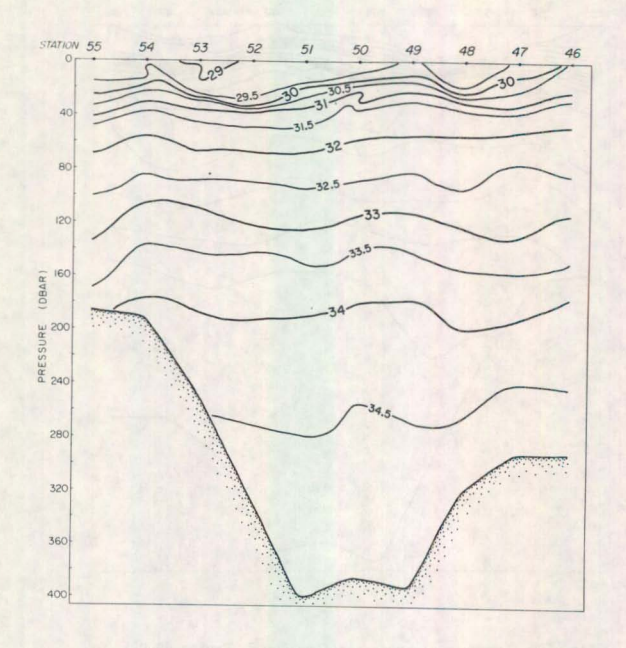


Fig. 70. Salinity cross-section, Row 7, Cruise 69-051.

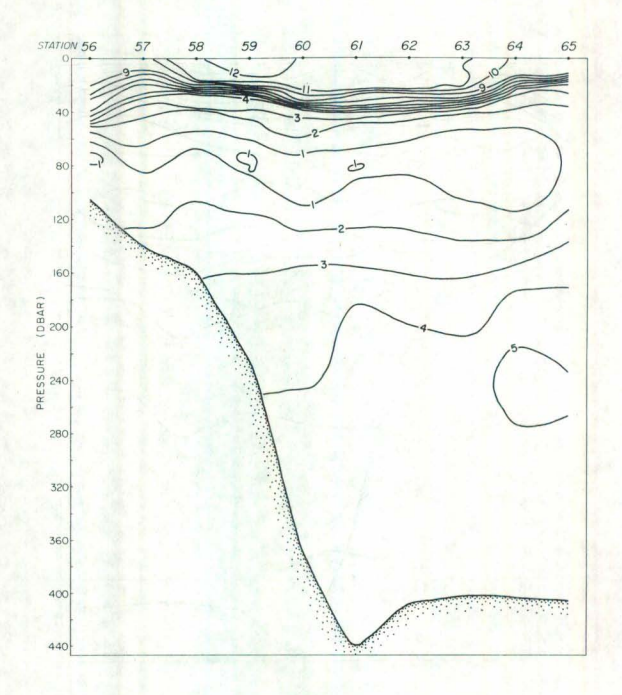


Fig. 71. Temperature cross-section, Row 8, Cruise 69-051.

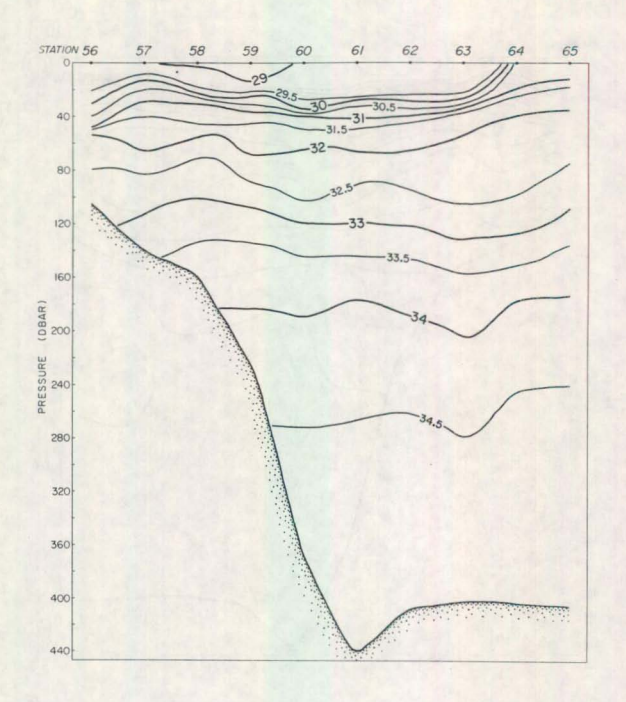


Fig. 72. Salinity cross-section, Row 8, Cruise 69-051.

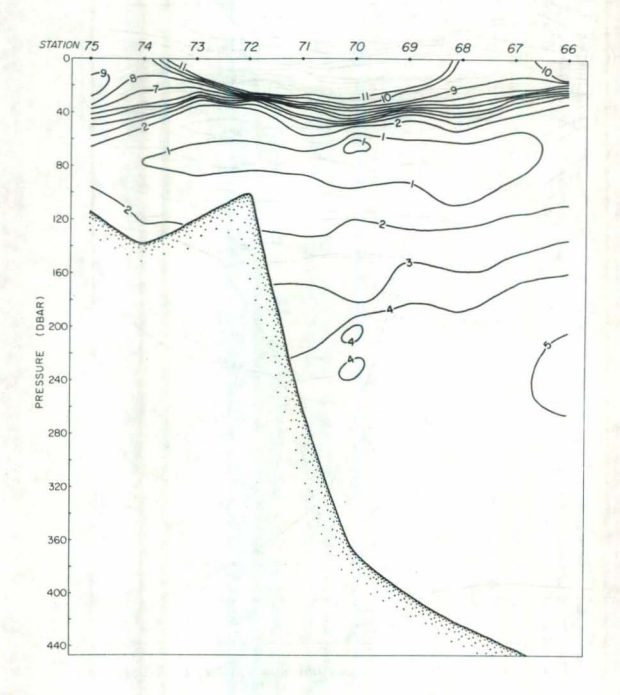


Fig. 73. Temperature cross-section, Row 9, Cruise 69-051.

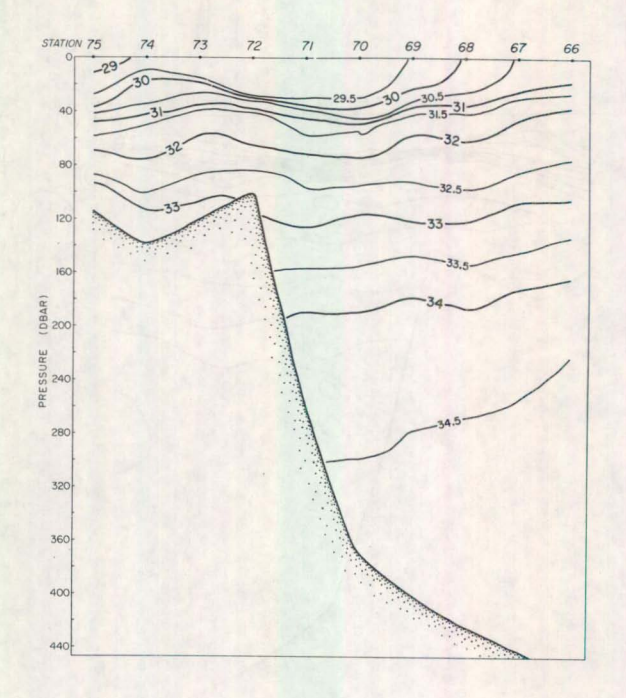


Fig. 74. Salinity cross-section, Row 9, Cruise 69-051.

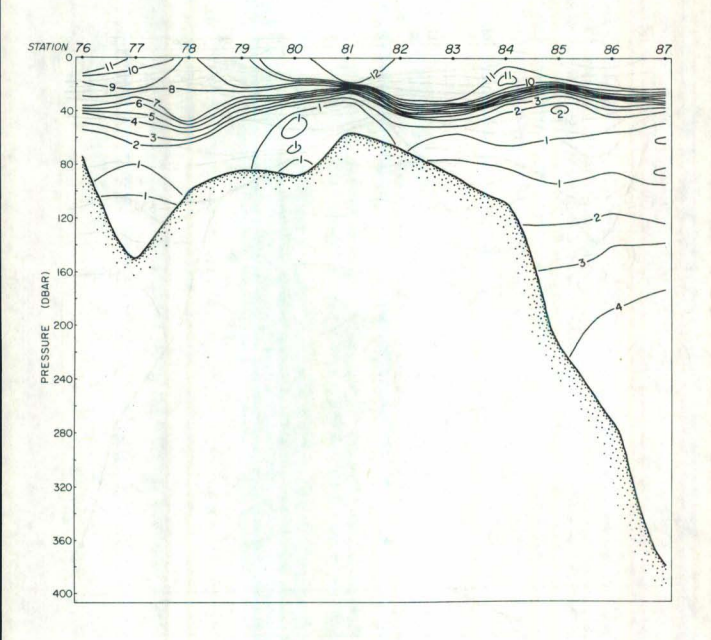


Fig. 75. Temperature cross-section, Row 10, Cruise 69-051.

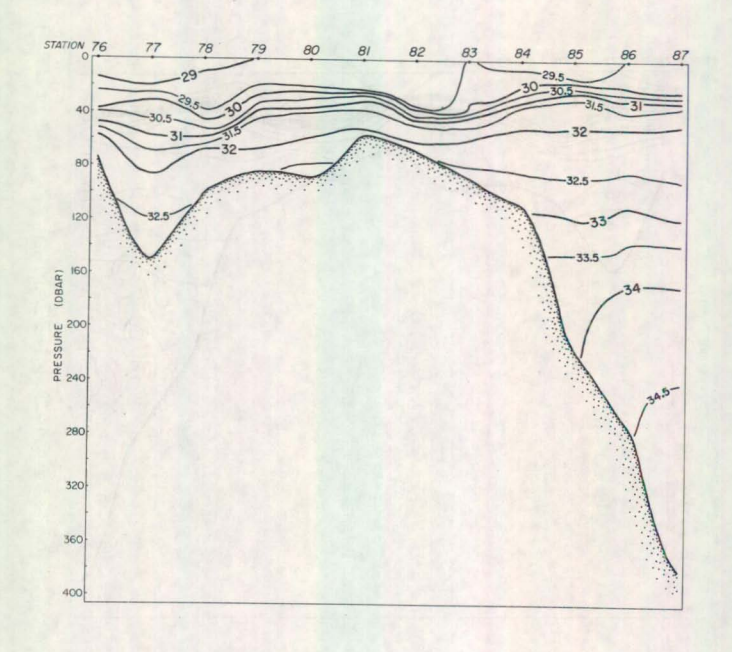


Fig. 76. Salinity cross-section, Row 10, Cruise 69-051.

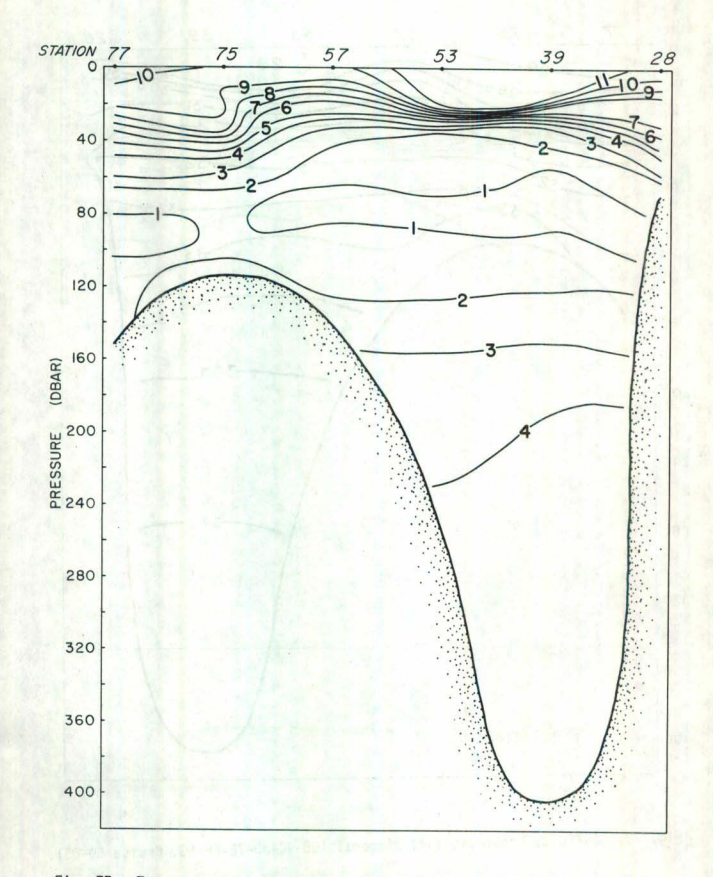


Fig. 77. Temperature cross-section, Diagonal 10B-9C-8D-7E-6F-5G, Cruise 69-051.

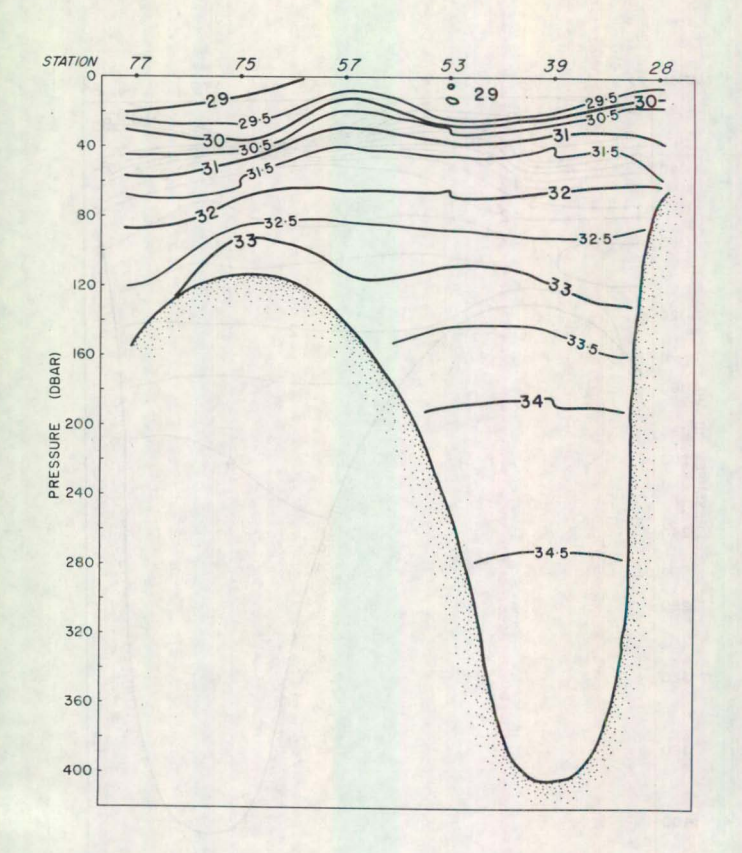


Fig. 78. Salinity cross-section, Diagonal 108-9C-8D-7E-6F-5G, Cruise 69-051.

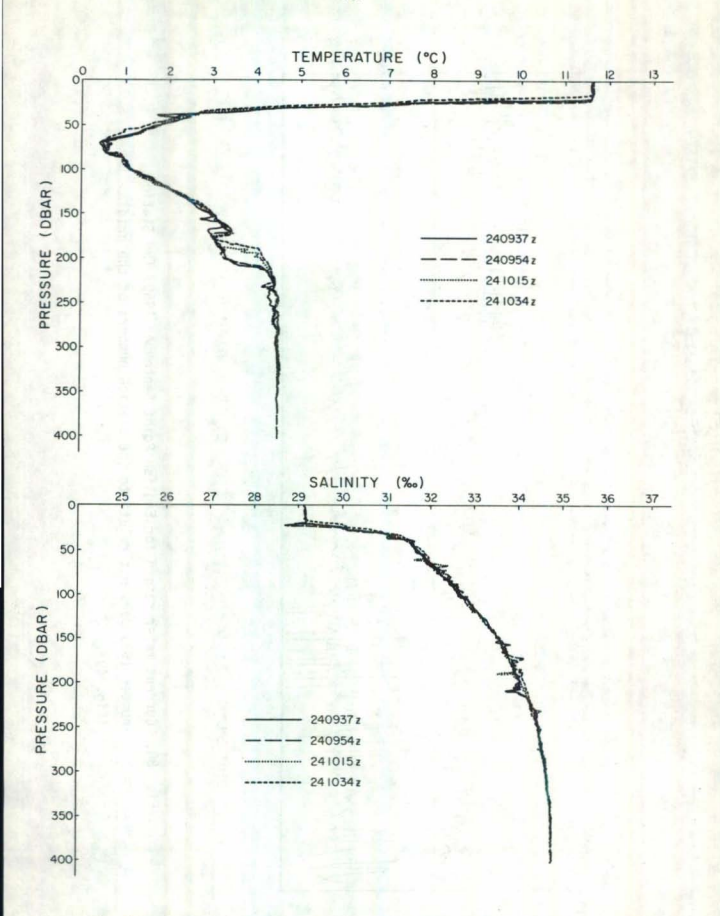


Fig. 79. Temporal variations in vertical temperature (top) and salinity (bottom) traces, Station 39, grid position 6F, Cruise 69-051.

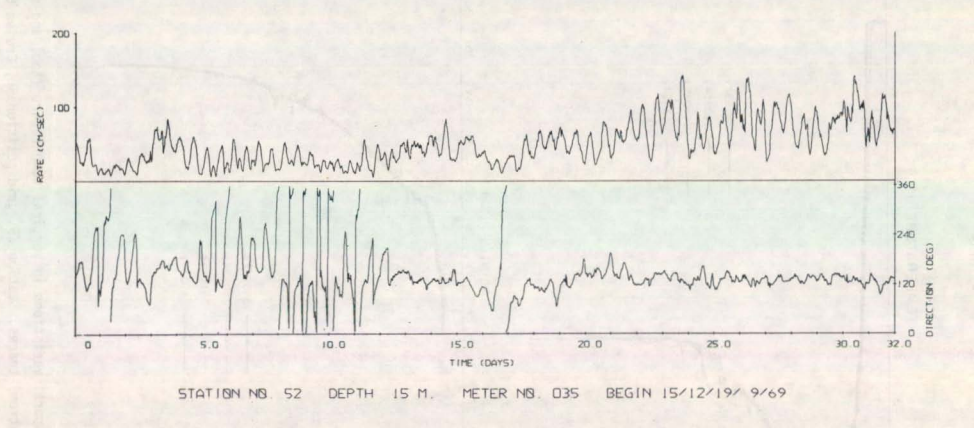


Fig. 80. Current meter record for English Point September 1969. The Station number (52) does not relate to the station numbers of the grid (Fig. 49).